

1 **Multivariate patterns between brain network properties,**
2 **polygenic scores, phenotypes, and environment in**
3 **preadolescents**

4
5 Jungwoo Seo¹, Eunji Lee², Bo-gyeom Kim², Gakyung Kim¹, Yoonjung Yoonie Joo³,
6 Jiook Cha^{1, 2, 4, 5}

7 1. Department of Brain and Cognitive Sciences, College of Natural Sciences,
8 Seoul National University, Seoul, South Korea

9 2. Department of Psychology, College of Social Sciences, Seoul National
10 University, Seoul, South Korea

11 3. Institute of Data Science, Korea University, Seoul, South Korea

12 4. Institute of Psychological Science, Seoul National University, Seoul, South
13 Korea

14 5. Graduate School of Artificial Intelligence, Seoul National University, Seoul,
15 South Korea

16

17 **Correspondence to:**

18 Jiook Cha, PhD

19 Gwanak-ro 1, Building 16, Suite M512, Gwanakgu, Seoul, 08826, South
20 Korea, connectome@snu.ac.kr

21

22 **Abstract**

23 The brain network is an infrastructure for cognitive and behavioral processes.
24 Genetic and environmental factors influence the development of the brain network.
25 However, little is known about how specific genetic traits and children's brain network
26 properties are related. Furthermore, insight into the holistic relationship of brain
27 network properties with genes, environment, and phenotypic outcomes in children is
28 still limited. To fill these knowledge gaps, we investigated the multivariate
29 associations between the brain network properties and three domains using a large
30 youth sample (the ABCD study, N=9,393, 9-10 years old): (i) genetic predisposition
31 of various traits, (ii) phenotypic outcomes, and (iii) environmental factors. We
32 constructed structural brain networks using probabilistic tractography and estimated
33 nodal and global network measures such as degree and network efficiency. We then
34 conducted sparse canonical correlation analysis with brain network measures and
35 polygenic scores of 30 complex traits (e.g., IQ), phenotypic traits (e.g., cognitive
36 ability), and environmental variables. We found multivariate associations of brain
37 network properties with (i) genetic risk for psychiatric disorders, (ii) genetic influence
38 on cognitive ability, and (iii) the phenotype of cognitive ability-psychopathology in
39 preadolescents. Our subsequent mediation analysis using the latent variables from
40 the canonical correlation analysis showed that the influence of genetic factors for
41 cognitive ability on the cognitive outcomes was partially mediated by the brain
42 network properties. Taken together, this study shows the key role of the development
43 of the brain structural network in children in cognitive development with its tight, likely
44 causal, relationship with genetic factors. These findings may shed light on future

- 45 studies of the longitudinal deviations of those gene-environment-brain network
- 46 relationships in normal and disease conditions.

47 Introduction

48 Childhood and adolescence are critical periods for brain development
49 (Bethlehem et al., 2022). Proper brain development during this time is vital for
50 cognitive and behavioral maturation (Bunge & Wright, 2007; Luna et al., 2010) and
51 mental health (Fornito et al., 2015; Paus et al., 2008). Such development is influenced
52 by genetic and environmental factors. Therefore, understanding the connections
53 between the brain, cognitive-behavioral traits in children, and the impact of genetics
54 and the environment on brain development is crucial in developmental and clinical
55 neuroscience. The Adolescent Brain and Cognitive Development (ABCD) study
56 (Jernigan et al., 2018) provides a rich dataset, encompassing genetic, neuroimaging,
57 environmental, and phenotypic data for over 10,000 children aged 9-10 years old at
58 baseline. This dataset opens an unprecedented opportunity to explore the connections
59 between genes, environment, brain, and phenotypic outcomes more robustly with less
60 concern about sampling bias (Marek et al., 2022) and age-confounding effects.

61 The brain is a complex network of tissues that communicate through white
62 matter bundles. Diffusion MRI and tractography enable the reconstruction of the
63 structural brain network (Jeurissen et al., 2019; Sotiropoulos & Zalesky, 2019). Graph
64 theory (Rubinov & Sporns, 2010) allows us to estimate the brain network properties
65 embedded in the whole brain's complex connectivity. The heritability of the brain
66 network properties in youth ranges from 25% to 70% (Koenis et al., 2015; van den
67 Heuvel, van Soelen, et al., 2013), indicating a strong genetic influence on shaping
68 brain networks. However, little is known about which specific genetic traits and
69 children's brain network properties are related. The recent development of the
70 polygenic score approach (Torkamani et al., 2018) has paved the way to quantify the

71 genetic propensity of specific traits, such as bipolar disorder, and explore which
72 genetic predispositions are related to the brain network properties.

73 Brain network properties are associated with cognitive abilities (Bathelt et al.,
74 2018; Kim et al., 2016; Koenis et al., 2015; Ma et al., 2017; Suprano et al., 2020),
75 psychiatric disorders (Alexander-Bloch et al., 2010; Collin et al., 2017; Rudie et al.,
76 2012), and environmental factors such as socioeconomic status (D. J. Kim et al., 2019;
77 Tooley et al., 2020) throughout the developmental period. Despite valuable insights
78 from previous studies, a comprehensive understanding of the holistic relationship of
79 brain network properties with genes, environment, and phenotypic outcomes in
80 children is still limited due to the predominant use of univariate approaches. No single
81 measurement is enough to characterize complex genes, brain networks, environment,
82 and phenotypes information. Rather, combining a range of variables can capture
83 complex traits more appropriately. Multivariate analysis, such as canonical correlation
84 analysis (CCA), is useful for investigating holistic relationships underlying a set of
85 variables simultaneously. CCA reveals multivariate associations linking sets of
86 variables from two domains by maximizing the canonical correlation between them
87 (Hotelling, 1936; Wang et al., 2020). For this reason, CCA has been extensively
88 employed in studying links between the brain, cognition, genes, and environment
89 (Alnaes et al., 2020; Fernandez-Cabello et al., 2022; Modabbernia et al., 2021; Smith
90 et al., 2015; Wang et al., 2020).

91 This study aims to investigate the multivariate associations between structural
92 brain network properties and three different domains in preadolescents: (i) genetic
93 predisposition of various traits, (ii) phenotypic outcomes, and (iii) environmental factors.
94 To achieve this, we leveraged the largest available childhood dataset (i.e., ABCD study)

95 and analysis techniques such as the polygenic score approach and sparse canonical
96 correlation analysis (Witten et al., 2009).

97

98 **Materials and Methods**

99 **ABCD participants**

100 We used genetic, neuroimaging, environmental, and phenotypic data from
101 the Adolescent Brain Cognitive Development (ABCD) study release 2.0 and 3.0
102 (<http://abcdstudy.org>). The ABCD study, which is the largest longitudinal investigation
103 of brain development and child health in the United States, recruited multiethnic
104 children (N=11,875) aged 9-10 years from 21 research sites with self-reported
105 ethnicities that comprised of 52.3% Caucasians, 20.3% Mexican Americans, 14.7%
106 African Americans, and 12.5% Asian-Americans and others. All participants and their
107 parents or legal guardians provided informed consent and assent forms before
108 participating in the study.

109

110 **Genotype Data**

111 The saliva DNA samples of study participants were collected, and 733,293
112 single nucleotide polymorphisms (SNPs) were genotyped at Rutgers University Cell
113 and DNA Repository (RUCDR) with Affymetrix NIDA Smoke Screen Array. We
114 excluded SNPs with genotype call rate <95%, sample call rate <95%, and minor
115 allele frequency (MAF) <1%. The genotypes were imputed using the Michigan
116 Imputation Server (Das et al., 2016) using the 1000 Genome phase3 version5 panel
117 (Genomes Project et al., 2015) with Eagle v2.4 phasing (Loh et al., 2016). Then, the
118 imputed variants with INFO score > .3 that did not meet our quality control criteria
119 (i.e., call rate <95%, MAF <1%, and Hardy–Weinberg equilibrium p-value <1e-6)

120 were additionally filtered out. To address potential bias derived from genetically
121 diverse and related family members in the ABCD study, we employed PC-Air
122 (Conomos et al., 2015) and PC-Relate (Conomos et al., 2016) to obtain genetically
123 unrelated individuals beyond 4th-degree relatives (i.e., kinship coefficient >0.022)
124 and to remove outliers beyond 6 SD limits from the center of ancestrally informative
125 principal component (PC) space. After quality control procedures, we included a total
126 of 11,301,999 variants in 10,199 unrelated multiethnic participants, among whom
127 7,893 participants were of European ancestry.

128

129 **Polygenic Scores (PGSs)**

130 We used publicly available European-based GWAS summary statistics to
131 calculate PGSs for 30 distinct traits: Attention-deficit/hyperactivity disorder (ADHD)
132 (Demontis et al., 2019), cognitive performance (CP) (Lee et al., 2018), educational
133 attainment (EA) (Lee et al., 2018), major depressive disorder (MDD) (Wray et al.,
134 2018), insomnia (Jansen et al., 2019), snoring (Jansen et al., 2019), intelligence
135 quotient (IQ) (Savage et al., 2018), post-traumatic stress disorder (PTSD) (Nievergelt
136 et al., 2019), depression (DEP) (Howard et al., 2019; Shen et al., 2020), body mass
137 index (BMI) (Akiyama et al., 2017; Locke et al., 2015), alcohol dependence
138 (ALCDEP) (Walters et al., 2018), autism spectrum disorder (ASD) (Grove et al.,
139 2019), automobile speeding propensity (ASP) (Akiyama et al., 2017), bipolar
140 disorder (BIP) (Stahl et al., 2019), cannabis during lifetimes (Cannabis) (Pasman et
141 al., 2019), ever smoker (Karlsson Linner et al., 2019), shared effects on five major
142 psychiatric disorder (CROSS) (Cross-Disorder Group of the Psychiatric Genomics,

143 2013), alcoholic drinks consumption per week (Drinking) (Karlsson Linner et al.,
144 2019), eating disorder (ED) (Watson et al., 2019), neuroticism (Nagel et al., 2018),
145 obsessive-compulsive disorder (OCD) (International Obsessive Compulsive Disorder
146 Foundation Genetics & Studies, 2018), first principal components of four risky
147 behaviors (Risky Behav) (Karlsson Linner et al., 2019), general risk tolerance
148 (RiskTol) (Karlsson Linner et al., 2019), schizophrenia (SCZ) (Bipolar et al., 2018;
149 Lam et al., 2019), worrying (Nagel et al., 2018), anxiety (Otowa et al., 2016),
150 subjective well-being (SWB) (Okbay et al., 2016), general happiness (UK Biobank
151 GWAS. Neale Lab. <http://www.nealelab.is/ukbiobank/>), and general happiness for
152 health (happiness-health) (UK Biobank GWAS. Neale Lab.
153 <http://www.nealelab.is/ukbiobank/>) and meaningful life (happiness-meaning) (UK
154 Biobank GWAS. Neale Lab. <http://www.nealelab.is/ukbiobank/>).

155 The GWAS summary statistics were used as input for PRS-CS (Ge et al.,
156 2019), a Bayesian regression method, to estimate the posterior effect sizes of SNPs.
157 The final scores were calculated using PLINK v1.9. To optimize the scores, we
158 followed the suggestion of the original PRS-CS paper and chose the optimal global
159 shrinkage hyperparameter (ϕ) from among four possible values: 1, 1e-2, 1e-4,
160 and 1e-6. The validation procedure was carried out within 14 PGSs (i.e., DEP, MDD,
161 ADHD, general happiness, happiness-health, happiness-meaning, SWB, insomnia,
162 snoring, BMI, PTSD, CP, EA, IQ) that had related measures in the ABCD study. For
163 each PGS, we performed linear regression of the phenotype variable with each of
164 the four scores and covariates (sex, age, and the first ten genetic PCs), and then,
165 based on R^2 and beta coefficient of PGS, selected one of the four PGSs. The
166 remaining 16 PGSs was automatically validated by PRS-CS-auto (Ge et al., 2019),

167 which select the optimal value of global shrinkage parameter employing a Bayesian
168 approach. Finally, to minimize the bias from population stratification, we residualized
169 the final PGSs with the first ten genetic PCs.

170

171 **Environmental Factors**

172 To investigate the relationship between children's brain network properties
173 and their environment, we examined 121 environmental and culture-related variables
174 for analysis. The variables consist of 80 variables representing the family history of
175 various problems (e.g., alcohol problem, drug use problem, depression, suicide-
176 related problem, etc.), 19 variables related to the residential history derived area
177 deprivation index (ADI), 11 parent characteristics and family culture related variables,
178 and others (e.g., perinatal condition, school environment, neighborhood safety, etc.).

179 To retain the sample as much as possible, we imputed missing values. For
180 categorical variables, we replaced the missing values with the most frequent value
181 (mode imputation); for continuous variables, with medians. Next, variables with near
182 zero variance were eliminated. We finally used 75 environmental variables for the
183 statistical analysis.

184

185 **Phenotype Data**

186 To investigate the relationship between children's brain network properties
187 and their mental health, physical health, and neurocognitive capacity, we examined
188 174 phenotypic variables. These included 89 mental health and abnormal behaviors

189 related variables (e.g., KSAD diagnosis, Child Behavior Checklist), 74 physical
190 health-related variables (e.g., physical disorders, medical history), and 10 NIH
191 Toolbox cognitive assessment variables and a delay discounting related variable
192 (i.e., cash choice task score). We also preprocessed the missing values with mode
193 imputation for categorical variables and median imputation for continuous variables.
194 Among phenotype data, variables having near zero variance were removed. We
195 finally used 117 phenotype variables for the statistical analysis after variable
196 selection based on the variance.

197

198 **Structural Brain Network Construction**

199 Detailed procedures for acquiring and preprocessing MRI data are described
200 in (Kim et al., 2022). To estimate brain structural networks from neuroimaging,
201 individual connectome data was generated. This was achieved by applying MRtrix3
202 (Tournier et al., 2019) to the preprocessed dMRI data to estimate whole-brain white
203 matter tracts and generate individualized connectomes. Probabilistic tractography
204 was performed using constrained-spherical deconvolution (CSD) (Calamante et al.,
205 2010; Tournier et al., 2007) with random seeding across the brain and target
206 streamline counts of 20 million. Initial tractograms were filtered using spherical-
207 deconvolution informed filtering (2:1 ratio)(Smith et al., 2013), resulting in a final
208 streamline count of 10 million. An 84x84 whole-brain connectome matrix was
209 generated for each participant using the T1-based parcellation and segmentation
210 from FreeSurfer with Desikan-Killiany atlas (Desikan et al., 2006)(68 nodes for the
211 cortical region and 16 nodes for the subcortical region). This approach ensured that

212 individual participants' connectomes were based on their neuroanatomy. The
213 computation was conducted on supercomputers at Argonne Leadership Computing
214 Facility Theta and Texas Advanced Computing Center Stampede2.

215

216 **Brain Network Measures (BNMs)**

217 We used the connectome matrix to construct an undirect weighted graph
218 representing the structural brain network. Nodes and edges in the graph represent
219 parcellated gray matter regions and connections between them, respectively.
220 Connection strength was quantified by the streamline count. To account for the
221 potential false positive connections generated by probabilistic tractography and their
222 impact on network topology, we eliminated extremely weak connections (streamline
223 counts less than 3). After thresholding, we excluded individuals with at least one
224 isolated node, assuming all brain regions are communicable via at least one path.

225 We calculated 18 different types of brain network measurements (BNMs)
226 representing different aspects of brain network's property (Rubinov & Sporns, 2010;
227 van den Heuvel & Sporns, 2011). We calculated eight global graph metrics (including
228 network density, modularity, normalized modularity, normalized average clustering
229 coefficient, normalized characteristic path length, global efficiency, normalized global
230 efficiency, small worldness) and five nodal graph metrics (including degree, strength,
231 clustering coefficient, betweenness centrality, nodal efficiency) to represent brain
232 network's global and regional properties. In addition, to examine rich club
233 organization, we also calculated raw and normalized rich club coefficient (van den
234 Heuvel & Sporns, 2011) of the network and the strength of rich club connection,

235 feeder connection, and local connection. Brain regions with top 12% degree were
236 defined as rich club nodes following previous work (van den Heuvel, Sporns, et al.,
237 2013). All graph measures were calculated using the package Brain Connectivity
238 Toolbox (<https://sites.google.com/site/bctnet/>).

239

240 **Sparse Canonical Correlation Analysis**

241 To examine a latent mode of covariation between structural brain network
242 properties and various polygenic scores, environmental factors, and phenotypic
243 outcomes, we used sparse canonical correlation analysis (Witten et al., 2009)
244 between brain network measures and three types of non-imaging data (i.e., PGSs,
245 environmental variables, phenotype variables) separately. Canonical correlation
246 analysis (CCA) is a multivariate procedure that maximizes the correlation between
247 the linear combinations of two sets of variables. Sparse canonical correlation
248 analysis is one of the popular variants of CCA with L1 regularization for sparse
249 solutions. We used sparse canonical correlation analysis to avoid over-fitting and
250 improve interpretability from sparse solutions.

251 The most popular algorithm for sparse canonical correlation analysis is
252 penalized matrix decomposition (PMD)(Witten et al., 2009), which solves
253 optimization problem of below equation for given two sets of data matrix $X_{n \times p}$, $Y_{n \times q}$.
254 (n: sample size; p, q: the number of variables of domain X and Y respectively; u, v:
255 canonical weights of domain X and Y respectively; c1, c2: regularization parameter)

$$256 \quad \max cov(Xu, Yv)$$

257 $s.t. \|u\|_2 = \|v\|_2 = 1, \|u\|_1 \leq c_1, \|v\|_1 \leq c_2$

258 To interpret Witten's sparse canonical correlation analysis as correlation
259 maximization, we need to assume covariance matrices $X^T X, Y^T Y$ are identity
260 matrices (Witten et al., 2009). But in our study with the high dimensional brain
261 datasets, the assumption is hardly satisfied (Fig. S1). For this reason, we interpreted
262 Witten's sparse canonical correlation analysis as a maximizing covariance algorithm
263 between two sets of variables rather than maximizing correlation.

264 To test generalizability of the sparse canonical correlation analysis results,
265 we split the dataset into a training and test set. For sparse canonical correlation
266 analysis with PGS and brain network measures, we split train set (n=5,411) and test
267 set (n=1,145) based on genetic relatedness to avoid including biological family in the
268 same dataset. In addition, we only used participants classified as genetically
269 European ancestry to control genetic confounding effects for sparse canonical
270 correlation analysis with PGSs. For sparse canonical correlation analysis with
271 environmental factors and phenotype data, we used stratified train (80%) - test
272 (20%) split by family history of various problems and KSAD diagnosis respectively.
273 **Table 2** summarizes the demographic information of the samples included in this
274 study.

275 We attempted to control the potential confounding effects by regressing out
276 the variance explained by age, sex, parental education, household income, marital
277 status, race ethnicity, BMI, and ABCD-site out of brain network measures,
278 environmental factors, and phenotype data. For binary variables such as family
279 history and KSADS-COMP, we regressed out with logistic regression. Residualized
280 data was used for the input of sparse canonical correlation analysis. On the other

281 hand, for polygenic scores, we did not regress out from PGSs because listed
282 covariates may not contaminate genetic information.

283 We selected optimal L1 regularization parameters from 5-fold cross validation
284 searching from 0.1 to 1 with a step size of 0.05 for both X and Y variables
285 respectively. The optimal L1 parameter combination was selected to maximize the
286 covariance of validation set between canonical variates of the first component (Fig.
287 S2).

288 For each sparse canonical correlation analysis, we extracted five modes of
289 covariance. To examine the statistical significance of each mode, we used a
290 permutation test. By randomly shuffling the rows of one dataset and remaining the
291 other, we generated 5,000 permutation sets. The p-value of each component was
292 calculated based on the number of permutation sets having greater covariance than
293 that obtained from the original dataset, and FDR-correction was done within each
294 CCA.

295
$$p_{uncorrected} = \frac{N_{null\ cov > cov}}{N_{null}}$$

296

297 Selected variables and their loading depend on the input sample. To find variables
298 reliably related to each mode, we used bootstrap resampling. We randomly
299 resampled 5,000 times with replacement and assessed the 95% confidence interval
300 of each variable's loading and how consistently it was selected. We interpreted the
301 significant modes based on loading patterns of variables whose 95% confidence
302 interval of loading does not cross zero (Xia et al., 2018) and selected more

303 frequently than expected by chance (i.e., more frequently selected than expected by
304 binomial distribution). Because sparse canonical correlation analysis with bootstrap
305 sample may change the order of components (axis rotation) and signs (reflection)
306 (Misic et al., 2016; Xia et al., 2018), the re-alignment procedure is needed to
307 estimate confidence interval of loading properly. We matched the components and
308 signs based on cosine similarity of weight vectors obtained from original dataset and
309 bootstrap sample. To assess the reproducibility of the findings, we applied the model
310 to the held-out test set and estimated significance of each mode through the
311 permutation test.

312

313 **Mediation Analysis**

314 After sparse canonical correlation analysis, we raised a hypothesis that the
315 genetic factors of cognitive ability may influence the phenotype of cognitive ability-
316 psychopathology through brain network properties (Results – Mediation Analysis). To
317 test the hypothesis, we examined whether brain network property scores related to
318 the genetic predisposition of cognitive ability (i.e., BNM score of PGS-BNM mode 2)
319 mediated the relationship between polygenic scores for cognitive ability (i.e., PGS
320 score of PGS-BNM mode 2) and the phenotype of cognitive ability-psychopathology
321 (i.e., phenotype score of Phenotype-BNM mode 2). Age, sex, race ethnicity, parental
322 education, household income, marital status, ABCD site, and BMI were used as
323 covariates in the mediation analysis. The two-sided p-values for each path were
324 estimated from 500 bootstrap samples.

325 Results

326 Modes of covariation between polygenic scores and structural brain network 327 properties

328 Using sparse canonical correlation analysis, we investigated the relationship
329 between 30 genome-wide polygenic scores (PGSs) and measures of brain network
330 properties (BNMs). Our analysis revealed a significant mode (mode 1) and a mode
331 that showed marginal significance (mode 2) (mode 1: $p = 0.006$, $cov = 0.846$, $r =$
332 0.107 ; mode 2: $p = 0.0545$ ($p_{unc} = 0.021$), $cov = 0.585$, $r = 0.118$, all p-values
333 were FDR corrected). Detailed results of the permutation test and the loading patterns
334 for all five modes can be found in the supplementary material (Fig. S3, S4).

335 The first mode of PGSs showed significant positive loadings for PGSs related
336 to psychiatric disorders, such as bipolar disorder and cross disorder (**Fig. 1a**). On the
337 brain side, normalized clustering and rich club coefficients showed positive loadings,
338 while network density, degree, and raw rich club coefficients, and the connection
339 strengths (among the bilateral rostral anterior cingulate, rostral middle frontal,
340 paracentral, lingual regions, and cerebellums) showed negative loadings (**Fig. 1b**,
341 **S4**).

342 In the second mode of the PGSs, we observed strong positive loadings for
343 PGSs related to cognitive abilities, such as cognitive performance (CP) and IQ.
344 Meanwhile, there were weak negative loadings for material use-related PGSs (**Fig.**
345 **1c**). In terms of corresponding brain network properties, positive loadings were found
346 for connection strength, betweenness centrality, normalized nodal efficiency of
347 middle temporal gyrus, and betweenness centrality of the left inferior parietal area.

348 On the other hand, the strength of posterior cingulate cortex, thalamus, and caudate,
349 as well as feeder and rich club connection strength had negative loadings (**Fig. 1d,**
350 **S4**). To sum up, the polygenic scores for higher cognitive ability were positively
351 linked to network integrity of the middle temporal gyrus and negatively associated
352 with connection strength of the posterior cingulate cortex, thalamus, and caudate.

353

354 **Modes of covariation between phenotypes and structural brain network** 355 **properties**

356 Among the five modes of covariation, only the second and the third mode were
357 significant and generalized to the hold-out test sets (mode 2: $p < 0.001$, $cov = 1.069$,
358 $r = 0.119$; mode 3: $p = 0.016$, $cov = 0.640$, $r = 0.089$, all p -values were FDR corrected).
359 We thus interpreted the second and third modes only. Detailed results of the
360 permutation test and the loading patterns for all five modes can be found in the
361 supplementary material (Fig. S5, S6).

362 The second mode of phenotypes depicted the covariation between brain
363 network properties and the shared characteristics of cognitive ability and
364 psychopathology (cognitive ability-psychopathology) (**Fig. 1e, 1f, S6**). Cognitive test
365 scores (i.e., NIH Toolbox scores) showed positive loadings, whereas
366 psychopathologic traits, such as CBCL and PGBI mania scores, showed negative
367 loadings. Several brain network properties showed loading patterns similar to that of
368 polygenic scores for cognitive ability (i.e., PGS mode 2). Consistent with the loadings
369 observed in PGS mode 2, the connection strength and nodal efficiency of the middle
370 temporal gyrus and betweenness centrality of the left inferior parietal region showed

371 positive loadings, while the strength of the posterior cingulate cortex, thalamus, and
372 caudate, along with the feeder and rich club connections, showed negative loadings.
373 Conversely, certain network properties were found to be statistically significant only
374 in relation to phenotypes. The nodal efficiency of the superior temporal region and
375 the betweenness centrality of the postcentral and supramarginal regions showed
376 positive loadings. Additionally, the strength of the anterior cingulate, paracentral, and
377 overall subcortical regions, as well as the nodal efficiency of the insula and
378 hippocampus, showed negative loadings. To summarize, phenotypes of cognitive
379 ability-psychopathology were positively associated with the network integrity of the
380 temporal and inferior parietal cortex, while being negatively associated with the
381 connection strength of the cingulate and subcortical regions.

382 Despite strong negative loadings in the NIH Toolbox scores, the third mode
383 did not show any significant features (Fig. S6).

384

385 **Modes of covariation between environmental factors and structural brain** 386 **network properties**

387 Among the five modes analyzed, the second mode showed a marginal level
388 of statistical significance, while the third mode showed a significant relationship
389 (mode 2: $p = 0.092$ ($p_{unc} = 0.0402$), $cov = 0.896$, $r = 0.074$; mode 3: $p = 0.016$,
390 $cov = 0.802$, $r = 0.124$, all p-values were FDR corrected). Further information
391 regarding the results of the permutation test and the loading patterns for all five
392 modes can be found in the supplementary material (Fig. S7, S8).

393 The second mode showed the relationship between environmental factors
394 related to socioeconomic status and brain network properties. Variables representing
395 socioeconomic advantages showed positive loadings, whereas variables
396 representing socioeconomic disadvantages showed negative loadings (**Fig. 2**).
397 Regarding its relationship with brain network properties, only the nodal efficiency of
398 the right hippocampus showed a significant association with the second mode (**Table**
399 **4**).

400 The third mode depicted the relationship between perinatal conditions, such
401 as caesarian section and age of parents, and brain network properties (**Fig. 2**).
402 Perinatal conditions showed positive associations with certain brain network
403 properties (**Table. 4**). Specifically, the connection strength, betweenness centrality,
404 and clustering coefficient of the entorhinal cortex showed positive loadings. In
405 contrast, the strength of the precentral gyrus, cerebellum, and thalamus, as well as
406 the nodal efficiency of the cerebellum and the degree of the caudate, showed
407 negative loadings.

408

409 **Mediation Analysis**

410 We discovered that both polygenic scores and phenotypes related to
411 cognitive ability shared covarying brain network properties. Specifically, we observed
412 shared brain network properties, including the connection strength and nodal
413 efficiency of the middle temporal gyrus, betweenness centrality of inferior parietal
414 regions, and the connection strength of the posterior cingulate cortex and thalamus
415 (**Fig. 1d, 1f**). These findings led us to the hypothesis that the genetic factors

416 influencing cognitive ability may exert their influence through brain network
417 properties.

418 To test this hypothesis, we examined whether the BNM score of PGS-BNM
419 mode 2 serves as a mediator between the PGS score of PGS-BNM mode 2 and the
420 phenotype score of phenotype-BNM mode 2 (**Fig. 3**). The result demonstrated that
421 brain network properties significantly mediated the relationship between polygenic
422 scores for cognitive ability and the phenotype of cognitive ability-psychopathology
423 (indirect effect = 0.013, $p < 0.001$).

424 Discussion

425 This study investigated the multivariate relationship of brain network
426 properties with genes, environment, and phenotypic outcomes in children. We
427 discovered multiple modes of covariation among the structural brain network
428 properties and the following factors: (i) the genetic propensity for psychiatric
429 disorders and cognitive capacity, (ii) the phenotypic outcomes related to the cognitive
430 ability and psychopathology, and (iii) the environmental factors, such as
431 socioeconomic status and perinatal conditions. Additionally, our study showed that
432 the brain network mediates the effects of the polygenic scores for cognitive capacity
433 on phenotypic outcomes of cognitive ability and psychopathology. This study offers
434 insight into which genetic factors are related to the brain network properties and the
435 multivariate relationships among variables of brain network properties, genes,
436 environmental factors, and phenotypic outcomes in children. It gives rise to
437 discussions about the underlying biology of brain network and cognitive development
438 and further hypotheses in this field.

439 In the sparse canonical correlation analysis with phenotypes, we observed
440 that the cognitive intelligence (NIH Toolbox) and psychopathology phenotypes
441 (CBCL) exhibited a single mode of covariation rather than distinct modes. This single
442 mode suggests that children's cognitive ability and abnormal behavior share
443 underlying brain network properties but with opposite signs of correlations. This
444 finding resembles previous findings, for instance, a single mode of positive-negative
445 behavioral and genetic traits covarying with brain connectivity (Smith et al., 2015;
446 Taquet et al., 2021).

447 Our mediation analysis showed that the brain network mediated genetic
448 predisposition and phenotypic outcomes of cognition and psychopathology during
449 childhood. This mediation may be facilitated by specific brain network properties
450 associated with both the polygenic scores for cognitive abilities and phenotypes
451 related to cognitive ability-psychopathology. Further investigation is necessary to
452 determine the extent of the involvement of these common network properties in the
453 gene-brain network-phenotypic outcome pathway. Mediation through the brain
454 network properties accounts for approximately 5% of the gene-phenotype pathway of
455 intelligence, implying other pathways, such as through cortical surface area or
456 thickness (Lett et al., 2020).

457 Children with higher polygenic scores for cognitive abilities or phenotype
458 scores of cognitive ability-psychopathology showed greater nodal efficiency in the
459 middle temporal gyrus and inferior parietal region. These regions are constituents of
460 the system proposed by the parieto-frontal integration theory (P-FIT) of intelligence
461 (Jung & Haier, 2007) and play a crucial role in semantic, language, and number
462 processing (Binder et al., 2009; Seghier, 2013; Visser et al., 2012). In contrast,
463 children with lower scores on cognitive ability-psychopathology exhibited greater
464 nodal efficiency in the hippocampus and insula. These regions have been implicated
465 in various cognitive functions, including learning, memory, emotional regulation, and
466 interoception (Jarrard, 1993; Namkung et al., 2017; Phelps, 2004; Rubin et al., 2014;
467 Sweatt, 2004). While previous studies have reported a positive correlation between
468 global efficiency and children's intelligence (Bathelt et al., 2018; Kim et al., 2016; Ma
469 et al., 2017), our results did not. Our study suggests that the relationship between
470 intelligence and network efficiency is more closely linked to the network efficiency of

471 some brain regions, such as the temporal and parietal regions, rather than the
472 overall global efficiency.

473 Our results indicate a negative association between the connection strength
474 of the posterior cingulate cortex and subcortical regions and polygenic scores and
475 phenotypes related to cognitive ability. During childhood and adolescence, FA of
476 white matter is known to increase (Tamnes et al., 2018). Unlike studies based on FA,
477 research has reported decreased streamline counts and density during this period,
478 particularly in connections with higher streamline counts and those linked to
479 subcortical regions (Baker et al., 2015; Lim et al., 2015). Considering these
480 documented changes in white matter connectivity, the observed negative association
481 may indicate a progression in white matter development among children with higher
482 cognitive abilities.

483 Our study suggests that children with higher polygenic scores for psychiatric
484 disorders have lower network density and degree across various brain regions.
485 Individuals with psychiatric disorders are known to have less white matter connection
486 (Chen et al., 2021; Perry et al., 2019; van den Heuvel & Fornito, 2014). These
487 findings suggest that the tendency of less white matter connections in individuals
488 with a higher genetic risk for psychiatric disorders is already observable in 9-10
489 years old. It is aligned with the findings that youth with higher genetic risks for
490 psychiatric disorders have smaller white matter volume and average connection
491 strength (Fernandez-Cabello et al., 2022; Taquet et al., 2021).

492 The wiring and maintenance of white matter tracts require significant
493 metabolic support. For this reason, the metabolic budget of the brain is a critical

494 factor in shaping the brain network (Bullmore & Sporns, 2012). Taking into account
495 network density is often used as a proxy for the wiring cost (Achard & Bullmore,
496 2007; Bassett et al., 2009), lower density observed in children with higher genetic
497 risks for psychiatric disorders may imply a link between genetic susceptibility to
498 psychiatric disorders and abnormal brain metabolism, subsequently affecting the
499 development of structural brain networks. Indeed, mitochondrial dysfunction has
500 consistently been proposed as a pathological foundation of psychiatric disorders
501 (Clay et al., 2011; Y. Kim et al., 2019; Rezin et al., 2009; Shao et al., 2008; Zuccoli et
502 al., 2017), and recent studies identified genetic overlaps between psychiatric
503 disorders and metabolic syndromes (Amare et al., 2017; Rodevand et al., 2021).

504 The brain network favors short-range connections over long-distance ones to
505 minimize wiring costs, promoting local segregation within the network (Bullmore &
506 Sporns, 2012). We observed a higher clustering coefficient in children with a higher
507 genetic risk for psychiatric disorders, which may be related to lower brain metabolic
508 support. Our results showed that genetic risks for psychiatric disorders were
509 negatively associated with raw rich club coefficients at $k=20-50$, but positively
510 associated with normalized rich club coefficients. Network density may partially
511 influence these correlations (van Wijk et al., 2010).

512 Our study indicates that environmental factors, such as socioeconomic status
513 and perinatal conditions, can affect brain network properties in children beyond mere
514 brain morphology (Alnaes et al., 2020). Specifically, we observed a positive
515 correlation between socioeconomic advantage and the nodal efficiency of the right
516 hippocampus. This finding aligns with previous studies showing the impact of
517 socioeconomic disadvantage on various aspects of the hippocampus, including gray

518 matter volume (Hanson et al., 2011; Jednorog et al., 2012), connectivity (Barch et
519 al., 2016), and network efficiency (D. J. Kim et al., 2019). However, the significant
520 associations between network properties and environmental factors were fewer in
521 number compared to genetic factors. This suggests that the influence of
522 environmental factors on brain network properties may be either less pronounced or
523 more heterogeneous than genetic factors.

524 This study has several limitations. Firstly, we used cross-sectional data,
525 which limits our ability to investigate the relationships between brain network
526 properties, genes, phenotypes, and the environment over time. Although our findings
527 provide insights into normative brain network development, a longitudinal study
528 design is necessary to fully understand developmental trajectories. Second,
529 polygenic scores only consider common genetic variants that reach a certain level of
530 statistical significance in a genome-wide association study (GWAS). Thus, polygenic
531 scores in this study do not capture the impact of rare variants or complex interactions
532 like gene-gene and gene-environment interactions. Lastly, our statistical models only
533 capture homogeneous linear relationships, which may not be adequate for
534 comprehending the complex interactions (Greene et al., 2022) that occur among
535 genetic profiles, environmental factors, phenotypic traits, and data-collection artifacts
536 within a large population study. The small effect sizes observed in the relationship
537 between brain network properties and genetic, phenotypic, and environmental
538 factors ($r = 0.074-0.124$) may indicate heterogeneous associations depending on
539 covariate profiles. To gain more informative insights into the relationships among
540 genes, environment, brain, and phenotypes, a more sophisticated model that can
541 capture heterogeneous associations based on covariates may be necessary. For

542 instance, employing conditional (or local) average treatment effect analysis with
543 causal machine learning (Athey et al., 2019) would be beneficial, as it would aid in
544 personal, clinical, and political decision-making.

545

546 **Data Availability**

547 All original data are publicly available from the NDA
548 (<https://nda.nih.gov/abcd/>). Mook data, which corresponds to the processed data
549 used in this study, was generated from conditional GAN for tabular data (Xu et al.,
550 2019) and are available from this site ([https://github.com/Transconnectome/ABCD-
551 brain-network-SCCA](https://github.com/Transconnectome/ABCD-brain-network-SCCA)).

552 **Code Availability**

553 Code is available from here: [https://github.com/Transconnectome/ABCD-
554 brain-network-SCCA](https://github.com/Transconnectome/ABCD-brain-network-SCCA).

555 **Funding**

556 This work was supported by the National Research Foundation of Korea
557 (NRF) grant funded by the Korea government (MSIT) (No. 2021R1C1C1006503,
558 2021K2A9A1A01102014, 2021K1A3A1A21037512, 2021M3E5D2A01022515), by
559 Seoul National University Research Grant in 2021 (No. 200-20210083), by Creative-
560 Pioneering Researchers Program through Seoul National University (No. 200-
561 20220046), by Semi-Supervised Learning Research Grant by SAMSUNG
562 (No.A0426-20220118), by Institute of Information & communications Technology

563 Planning & Evaluation (IITP) grant funded by the Korea government(MSIT)
564 [NO.2021-0-01343, Artificial Intelligence Graduate School Program (Seoul National
565 University)], and by Identify the network of brain preparation steps for concentration
566 Research Grant by Looxid Labs (No.339-20230001).

567

568 **Author contributions**

- 569 ● Jungwoo Seo, Conceptualization, Data curation, Formal analysis, Validation,
570 Investigation, Visualization, Writing – original draft, Writing – review and editing
- 571 ● Eunji Lee, Data curation, Writing – original draft, Writing – review and editing
- 572 ● Bogyom Kim, Data curation, Writing – review and editing
- 573 ● Gakyung Kim, Data curation, Writing – original draft, Writing – review and editing
- 574 ● Yoonjung Yoonie Joo, Data curation, Writing – review and editing
- 575 ● Jiook Cha, Conceptualization, Supervision, Project administration, Funding
576 acquisition, Resources, Data curation, Writing – original draft, Writing – review and
577 editing.

578 **Ethics**

579 **Competing Interest Disclosures**

580 None of the authors have significant competing financial, professional, or personal
581 interests that might have influenced the performance or presentation of the work
582 described in the manuscript.

583

584

585 **Tables**

586 **Table 1. Abbreviation of PGSs and their meaning.**

Abbreviation	Meaning
CROSS	Cross disorder between ASD, ADHD, bipolar disorder, MDD, and schizophrenia
Neuroticism	Neuroticism
Risky Behav	The first principal component of the four risky behaviors
RiskTol	General risk tolerance
Worry	Worrying subtype
ASP	Automobile speeding propensity: the tendency to drive faster than the speed limit
ALCDEP	Alcohol dependence
ED	Eating Disorder (Anorexia nervosa)
Drinking	Drinks per week – the average number of alcoholic drinks consumed per week
ASD	Autism Spectrum Disorder
BIP	Bipolar disorder
Cannabis	Cannabis during their lifetime (self-reported)
Smoke	Ever smoker – whether one has ever been a smoker
SCZ	Schizophrenia
OCD	Obsessive-Compulsive Disorder

Anxiety	Anxiety
DEP	Depression
MDD	Major Depression Disorder
GHapi	General Happiness
GHapiHealth	General Happiness - health
GHapiMean	General Happiness - meaningful life
SWB	Subjective Well Being
INSOMNIA	Insomnia
SNORING	Snoring
BMI	Body Mass Index
PTSD	Post-Traumatic Stress Disorder
CP	Cognitive Performance
EA	Education Attainment
IQ	Intelligence Quotient
ADHD	Attention-Deficit/Hyperactivity Disorder

587

588

589

Table 2. Demographic information of the study participants.

		PGS – BNM (n=6,549)		ENV – BNM (n=9,393)		Pheno – BNM (n=8,895)	
		train	test	train	test	train	test
N	total	5,406	1,143	7,514	1,879	7,116	1,779
Sex	Male	2,869	600	3,931	965	3,741	905
	Female	2,537	543	3,583	914	3,375	874
Race	White	3,831	865	4,167	1,041	4,086	1015
	Black	34	7	995	234	866	221
	Hispanic	993	154	1,406	401	1,269	323
	Asian	6	1	147	32	143	29
	Other	542	116	799	171	752	191

590

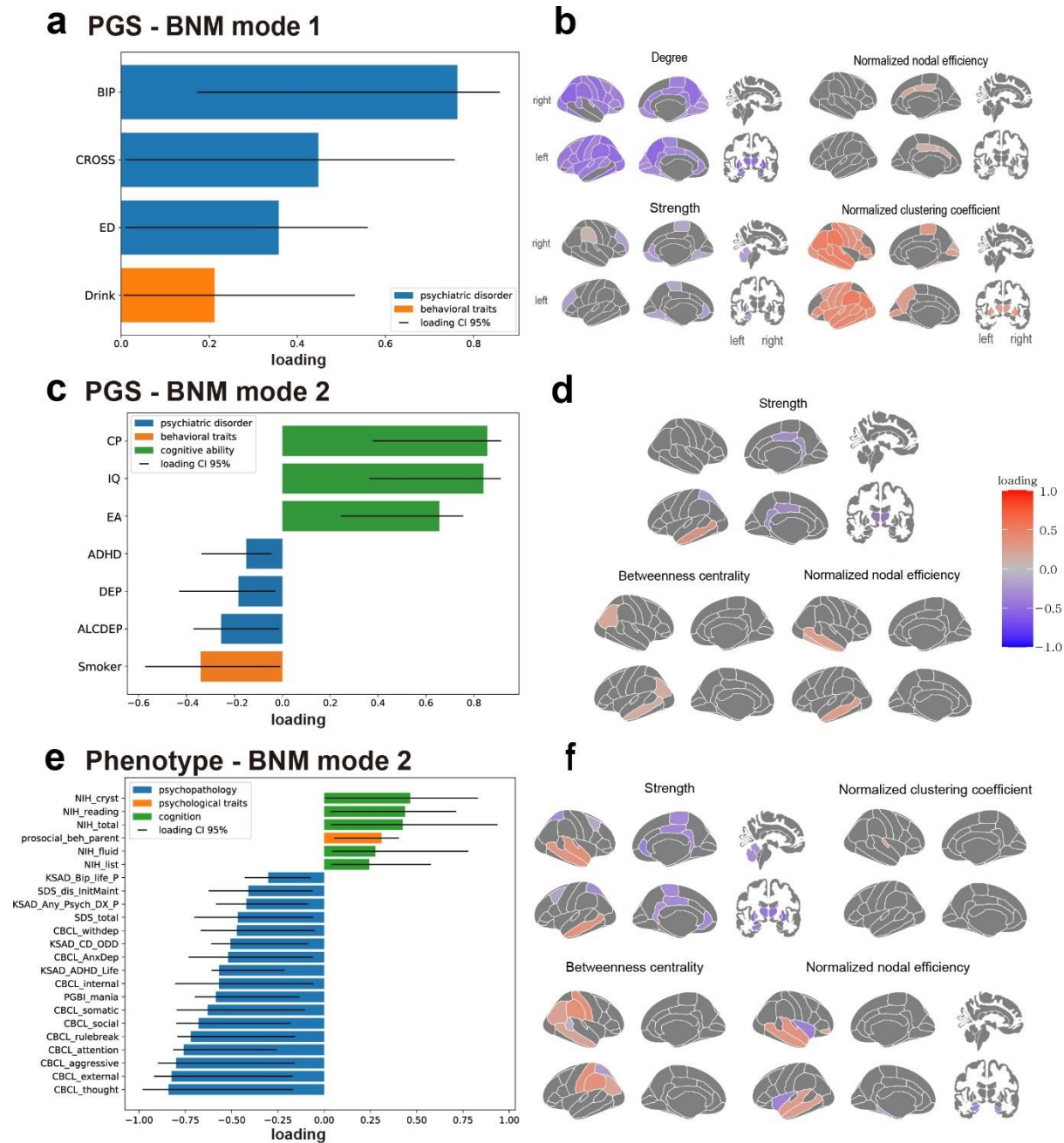
591 **Table 3. p-value, correlation coefficient, covariance of sparse**
 592 **canonical correlation analysis results.** p-value of each mode is estimated by
 593 permutation test. * p_FDR < 0.05, ** p_FDR < 0.01, *** p_FDR < 0.001, † p_uncorrected < 0.05.

Sparse Canonical Correlation Analysis with Brain Network Metrics		Mode1	Mode2	Mode3	Mode4	Mode5
Polygenic Scores	p_training	0.0060**	0.0545 (0.0218)†	0.6633	0.9640	0.3033
	p_test	0.0060**	0.0210*	0.4582	0.1587	0.4582
	corr	0.1071	0.1176	0.1231	0.0831	0.1404
	cov	0.8458	0.5845	0.4425	0.3517	0.3830
Phenotypes	p_training	0.0020*	<0.001***	0.0160*	0.2128	0.0678
	p_test	0.1020	0.0060**	0.0110*	0.1990	0.5814
	corr	0.1124	0.1194	0.0885	0.0924	0.1233
	cov	1.2243	1.0692	0.6401	0.4819	0.4593
Environmental Factors	p_training	0.0920	0.0920 (0.0402)†	0.0160*	0.5582	0.0920
	p_test	0.1227	0.0145*	0.0030**	0.4682	0.3663
	corr	0.0745	0.0741	0.1239	0.0843	0.1060
	cov	1.1196	0.8956	0.8023	0.5263	0.5226

595 **Table 4. Sparse canonical correlation analysis results of**
 596 **environmental factors-brain network measures.** Only significant brain network
 597 measures are presented. The loadings of corresponding environmental factors are visualized in
 598 Figure 2.

	Region	Network measure	Loading	Loading 95% CI
Mode 2	Hippocampus	Nodal efficiency R-HI	0.2098	[0.0031, 0.4603]
Mode 3	Caudate	Deg L-CA	-0.3778	[-0.4016, -0.0038]
		Deg R-CA	-0.3753	[-0.3930, -0.0156]
	Entorhinal cortex	Stren L-EC	0.3417	[0.0336, 0.4331]
		Stren R-EC	0.3483	[0.0378, 0.4348]
		BC_L-EC	0.1091	[0.0174, 0.1560]
		Norm_clust_coef L-EC	0.3691	[0.0208, 0.4188]
		Norm_clust_coef R-EC	0.3879	[0.0357, 0.4383]
	Precentral gyrus	Stren L-PrCG	-0.4642	[-0.4978, -0.0116]
		Stren R-PrCG	-0.4356	[-0.4866, -0.0100]
	Cerebellum	Stren L-CER	-0.2761	[-0.3509, -0.0222]
		Stren R-CER	-0.2768	[-0.3465, -0.0171]
		Nodal efficiency L-CER	-0.3695	[-0.4661, -0.0615]
		Nodal efficiency R-CER	-0.3699	[-0.4646, -0.0603]
	Thalamus	Stren L-TH	-0.4175	[-0.5760, -0.0779]
Stren R-TH		-0.4141	[-0.5797, -0.0651]	

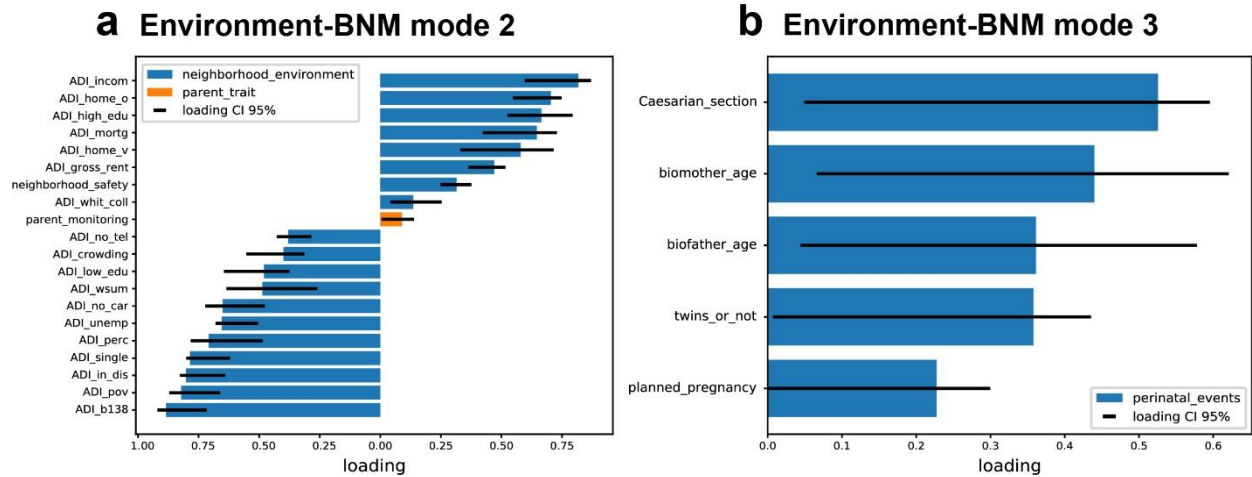
	Temporal pole	Stren R-TP	0.1590	[0.0255, 0.2223]
		Norm_clust_coef L-TP	0.3942	[0.0216, 0.4324]



600

601 **Figure 1 Sparse canonical correlation analysis results of polygenic scores-brain network**
 602 **measures and phenotypes-brain network measures.** The results of the first and second modes of
 603 polygenic scores (PGSs) - brain network measures (BNMs) and the second mode of phenotypes -
 604 brain network measures. (a) The loadings of significant PGS variables in the PGSs-BNMs mode 1.
 605 The error bars represent the 95% confidence interval of the loading, estimated from the 5,000
 606 bootstrap samples. Among the 30 PGSs, only significant PGS variables are presented, while the
 607 others can be found in supplementary figure 4. The color of each bar represents the category to which

608 the variable belongs. (Abbreviations - BIP: bipolar disorder; CROSS: cross-disorder; ED: eating
609 disorder; Drink: drink per week) (b) The loadings of significant nodal brain network measures in the
610 PGSs-BNMs mode 1. The loading patterns were visualized with R-package 'ggseg' (Mowinckel &
611 Vidal-Pineiro, 2020) (c) The loadings of significant PGS variables in the PGSs-BNMs mode 2.
612 (Abbreviations - CP: cognitive performance; EA: educational attainment; DEP: depression; ALCDEP:
613 alcohol dependence; Smoker: ever smoking) (d) The loadings of significant nodal brain network
614 measures in the PGSs-BNMs mode 2. (e) The loadings of significant PGS variables in the
615 phenotypes-BNMs mode 2. The loading patterns of other modes are shown in supplementary figure 6
616 (abbreviations- NIH: NIH Toolbox score; KSAD: K-SADS (Kiddie Schedule for Affective Disorders and
617 Schizophrenia; SDS: sleep disturbance scale; CBCL: child behavior checklist; PGBI: parent version of
618 general behavior inventory) (f) The loadings of significant nodal brain network measures in the
619 phenotypes-BNMs mode 2.
620



621

622 **Figure 2 Sparse canonical correlation analysis results of environmental factors-brain network**

623 **measures.** (a) The loadings of environmental variables in mode 2. (b) The loadings of environmental

624 variables in mode 3. Only significant variables are presented. The loadings of corresponding brain

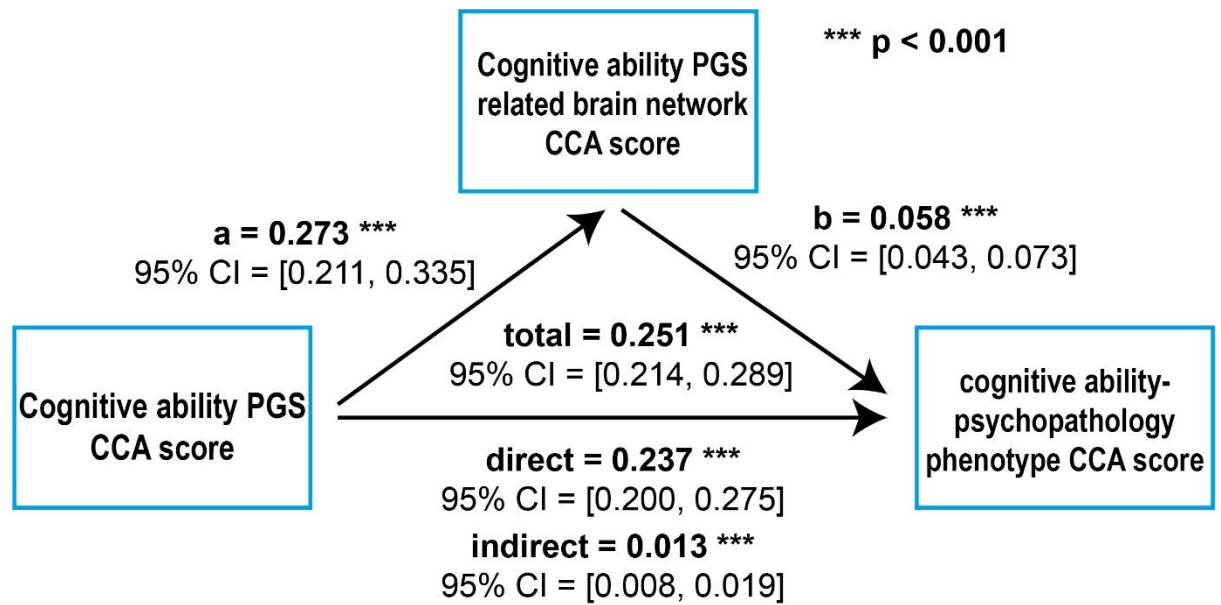
625 network measures are presented in Table 4, and the loading patterns of other modes are shown in

626 supplementary figure 8 (abbreviation – ADI: residential history derived area deprivation index)

627

628

629



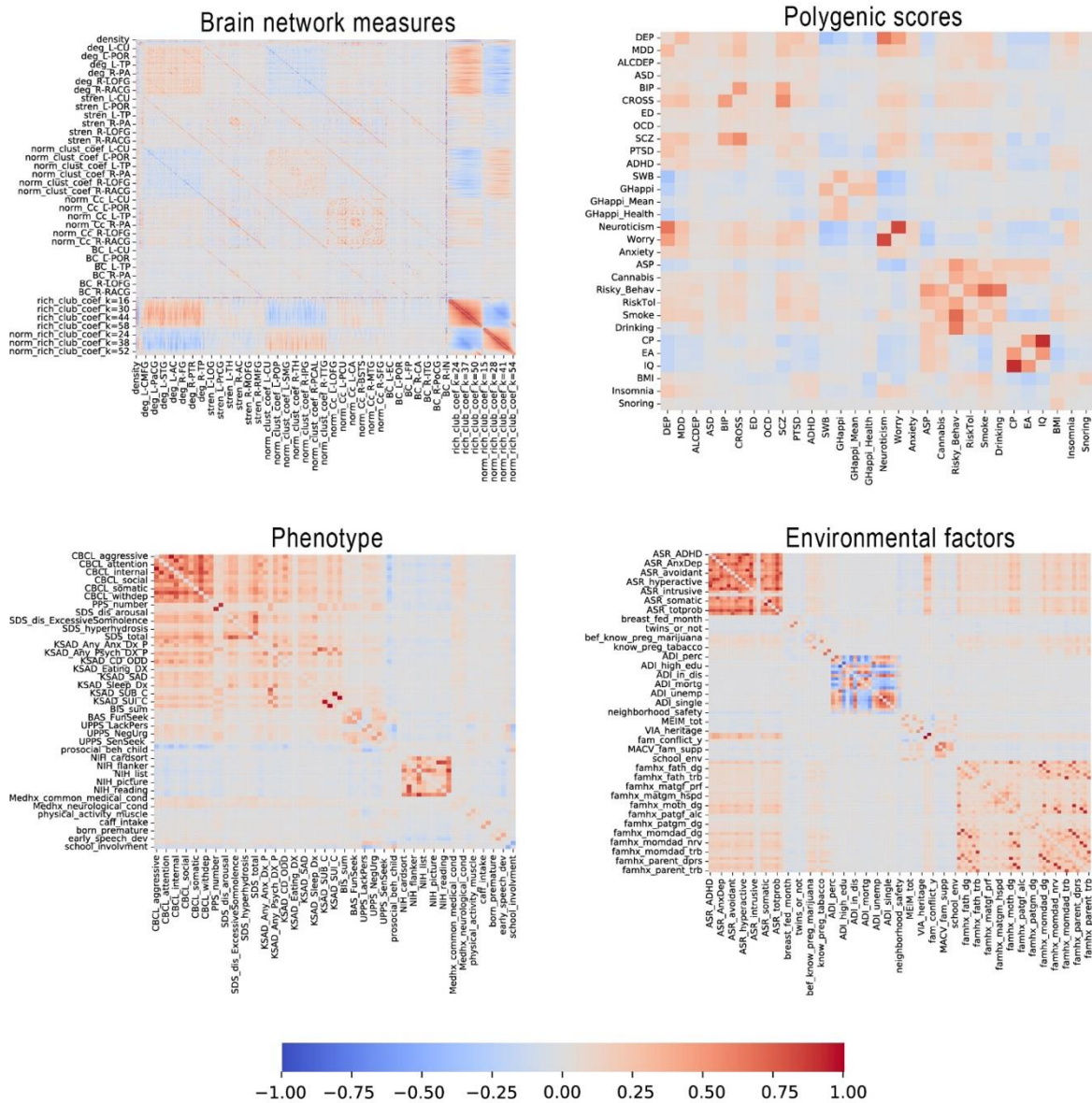
631 **Figure 3 Result of mediation analysis.** We used cognitive ability PGS CCA score (i.e., PGS CCA
632 score of PGS-BNM mode 2) as an independent variable, brain network property CCA score related to
633 the cognitive ability PGS (i.e., BNM CCA score of PGS-BNM mode 2) as a mediator, and phenotype
634 of intelligence-psycho pathology CCA score (i.e., phenotype CCA score of Phenotype-BNM mode 2)
635 as a dependent variable. The p-value and effect size of all paths were presented.

636

637

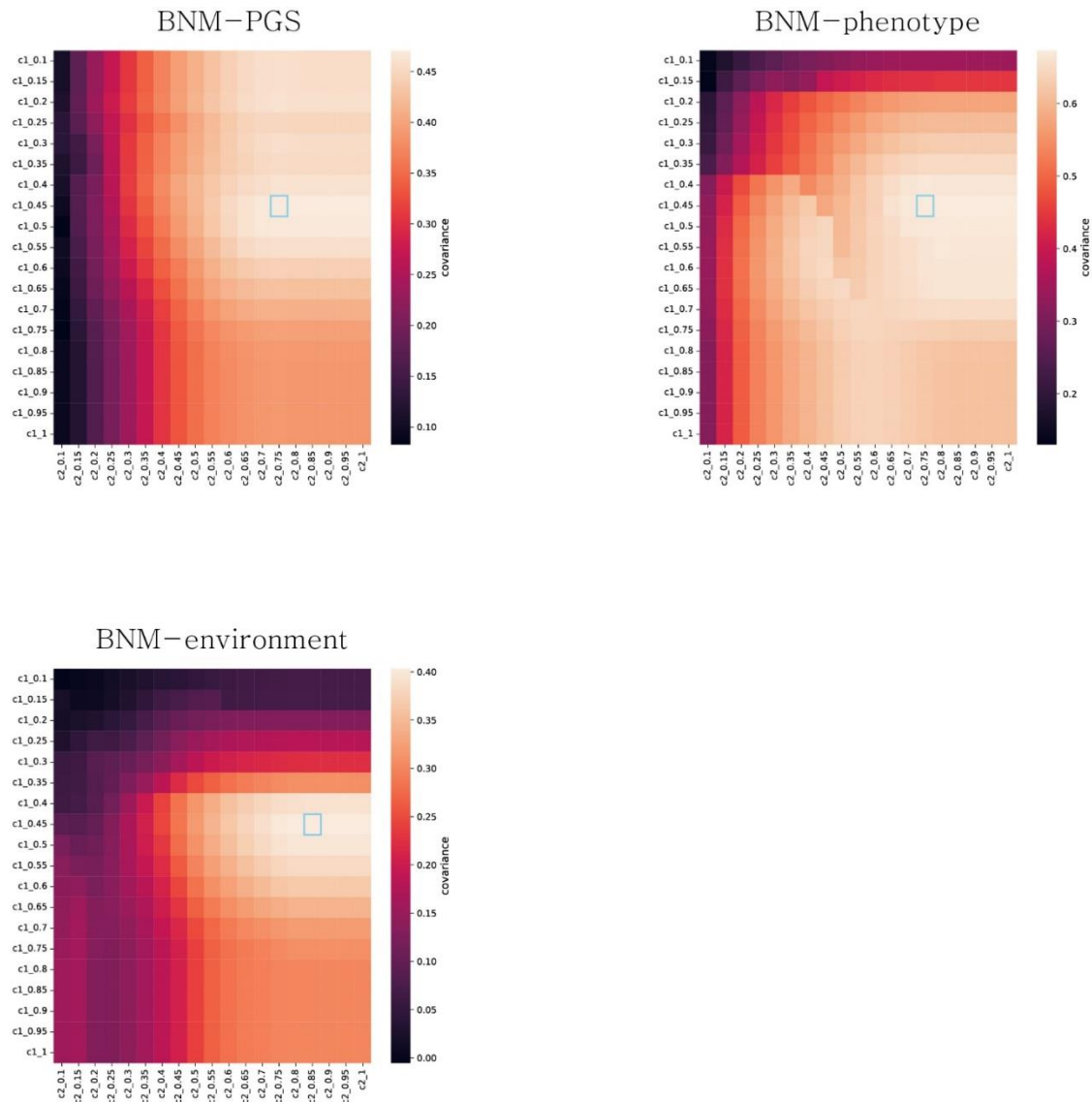
638 **Supplementary Materials**

639



640
641
642
643

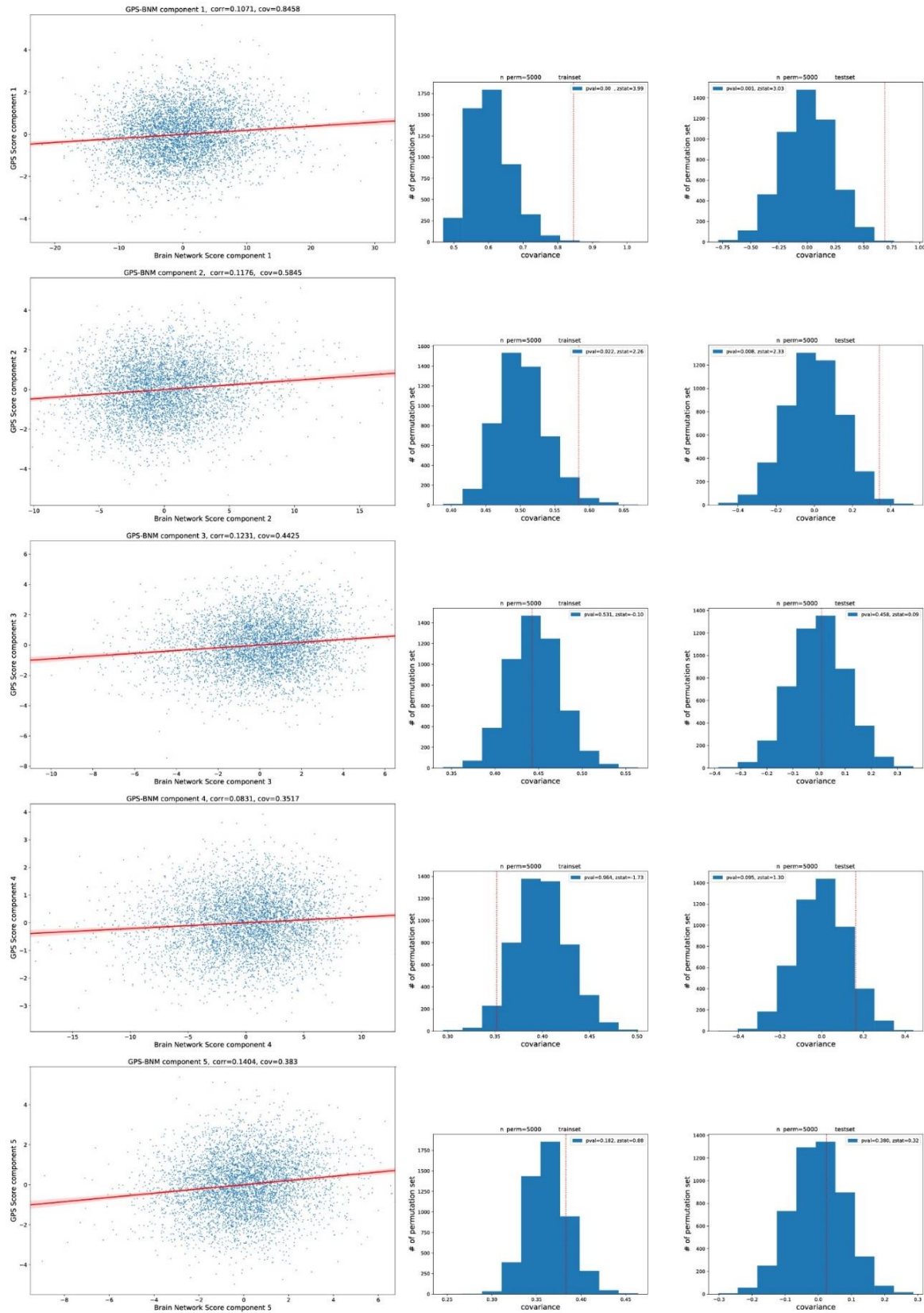
Supplementary Figure 1. Check Witten's assumption. $\frac{1}{n} \mathbf{X}^T \mathbf{X} - \mathbf{I}$ of the analyzed data is presented. Here, X represents the data from which the variance explained by covariates has been regressed out, as mentioned in the main text.



644

645 **Supplementary Figure 2. Optimal regularization parameters.** We conducted a grid search to
646 optimize the L1 regularization parameters for Sparse Canonical Correlation Analysis (SCCA). The grid
647 search ranged from 0.1 to 1 in sparsity parameters, with increments of 0.05. The objective was to
648 identify the sparsity parameter pair that yielded the highest mean covariance of the first component in
649 the validation set, using 5-fold cross-validation.

650



651

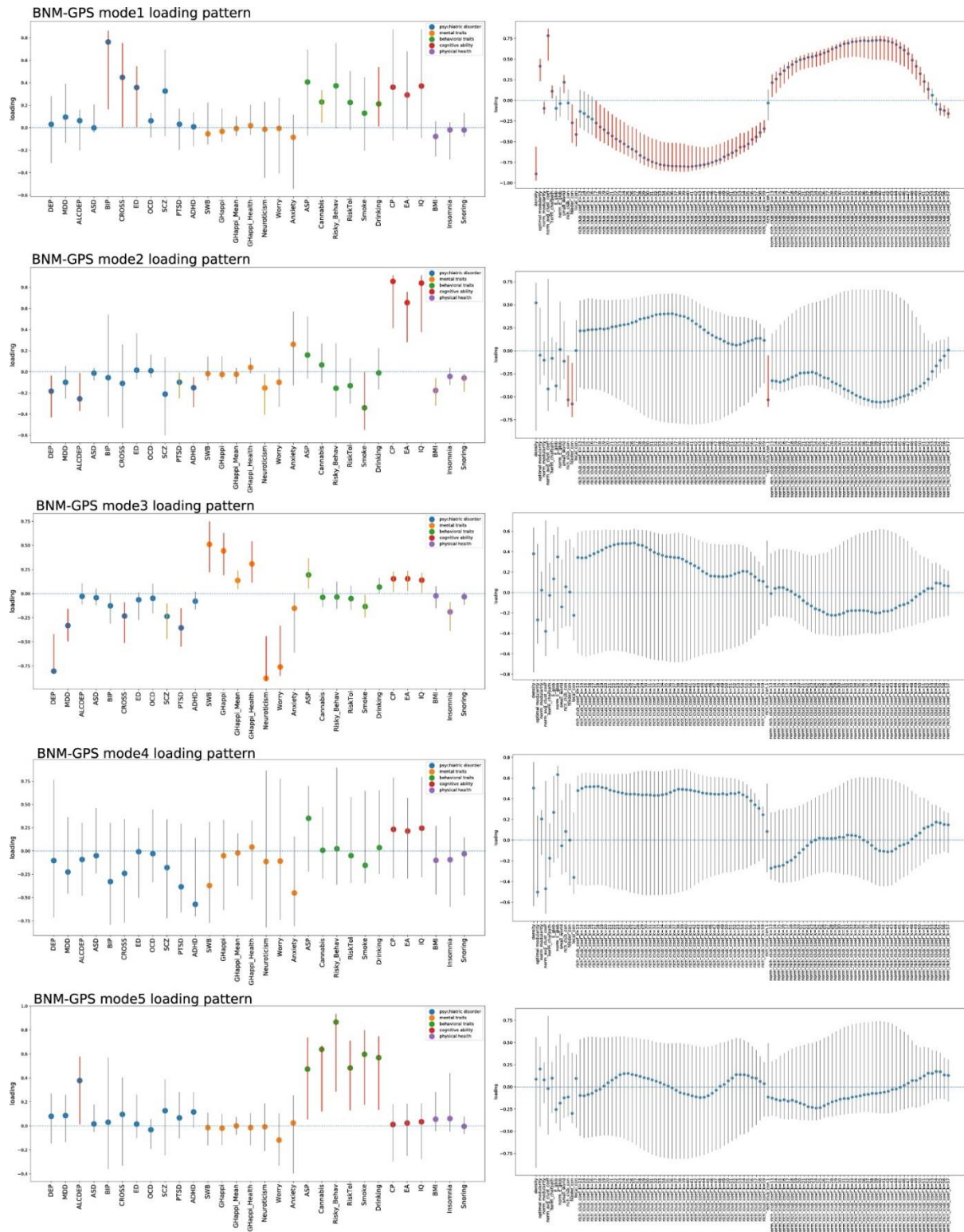
652 **Supplementary Figure 3. Scatter plots of SCCA scores of brain network measures versus**
 653 **SCCA scores of polygenic scores and their permutation test results of training and test set.**

654 Each permutation test result shows the null distribution of SCCA estimated by permutation test.

655 Dashed red line refers to the actual covariance of each mode.

656

657



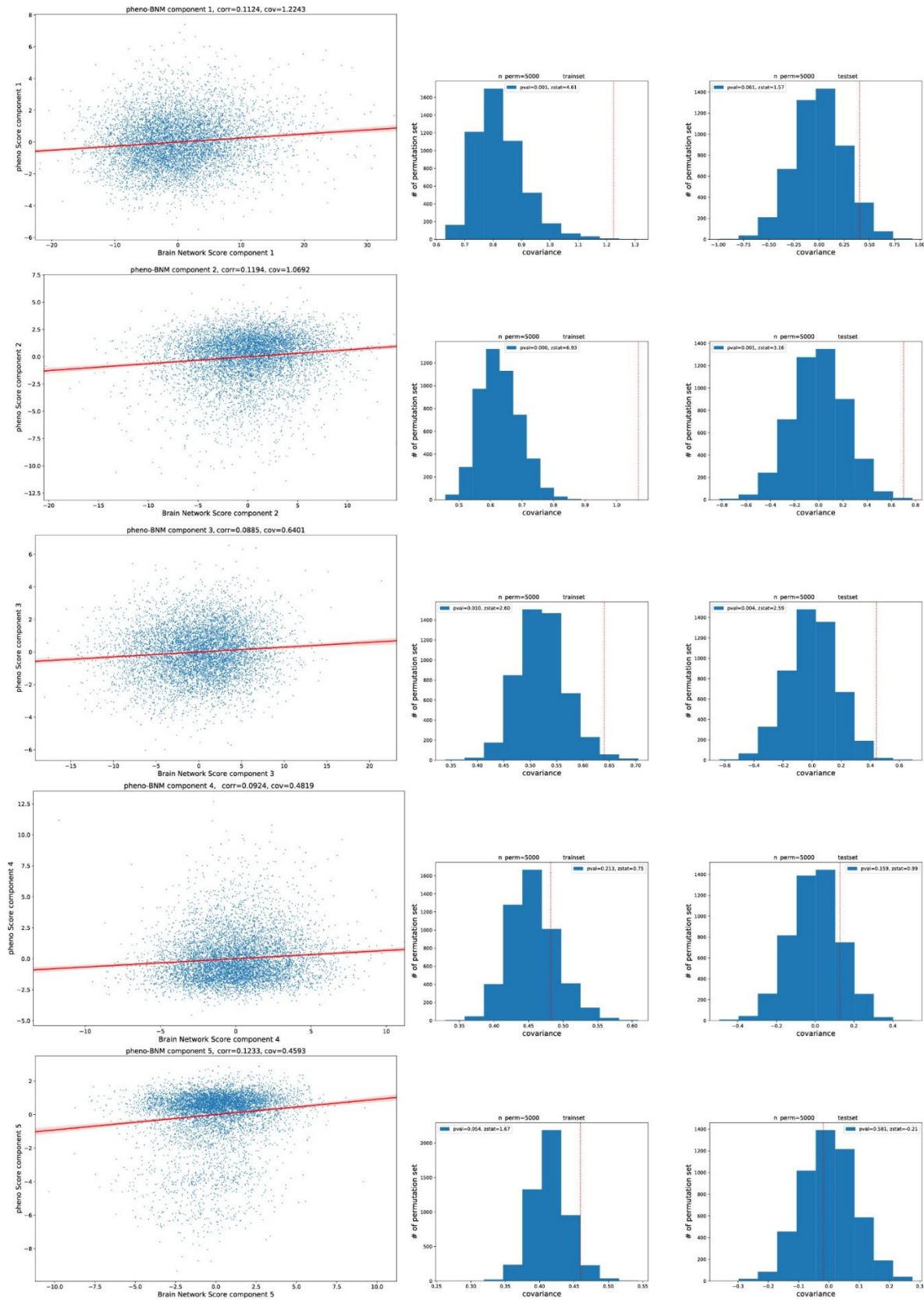
658

659 **Supplementary Figure 4. Sparse CCA loading patterns of brain network measures – polygenic**

660 **scores.** The left column presents the loading of each polygenic score variable, while the right column

661 displays the loadings of global brain network measures and rich club coefficients. Each data point

662 represents the loading value of a specific variable and is color-coded based on its category. The error
663 bars indicate the 95% confidence interval of the loading, which was estimated using bootstrapping.
664 Gray-colored error bars indicate a 95% confidence interval that crosses 0. Yellow-colored error bars
665 indicate a 95% confidence interval that does not cross 0 but corresponds to a variable that is not
666 frequently selected by Sparse CCA. Red-colored error bars represent a 95% confidence interval that
667 does not cross 0 and indicates a variable that is frequently selected. Only the variables represented
668 by red error bars are presented in the main text.



669

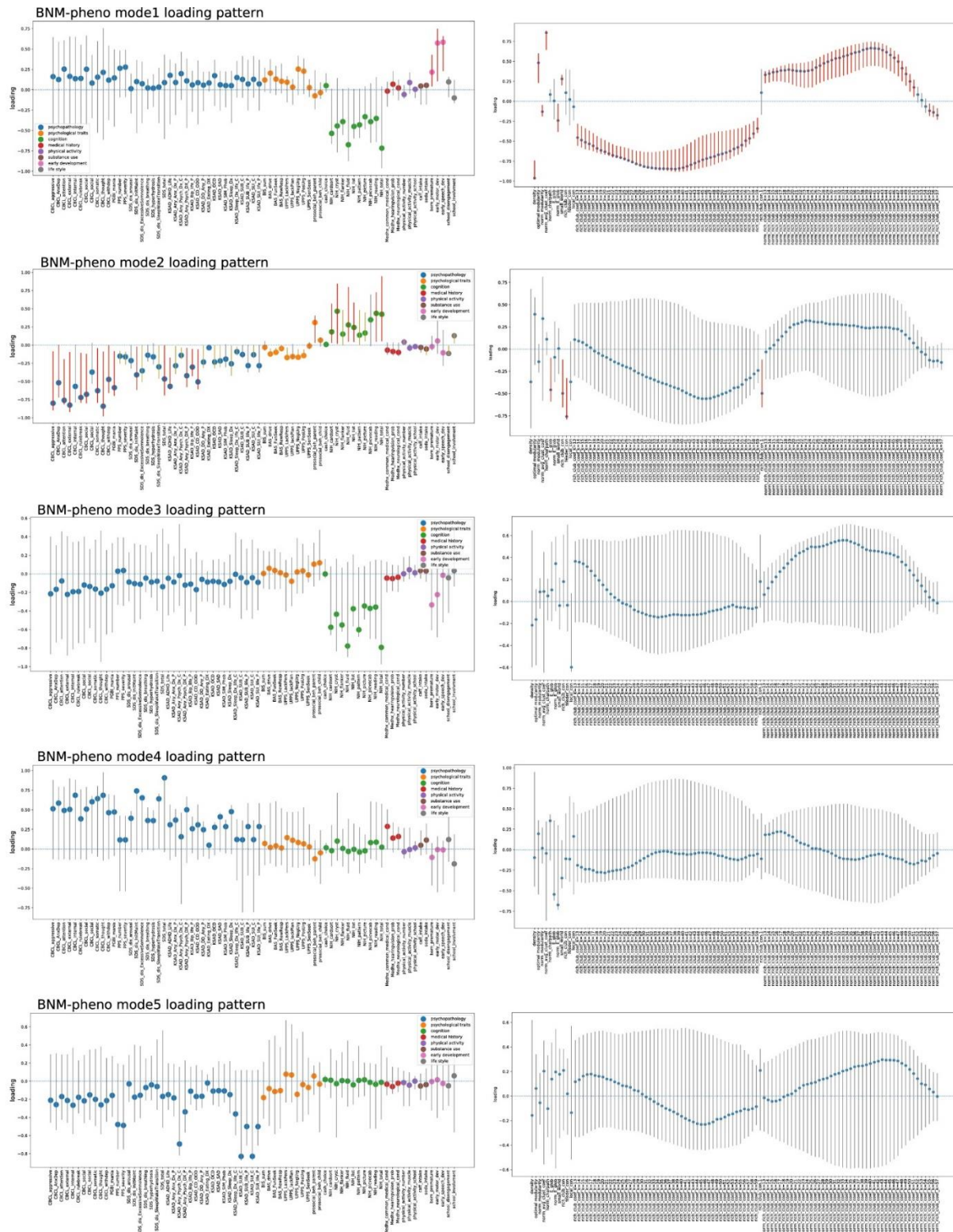
670 **Supplementary Figure 5. Scatter plots of SCCA scores of brain network measures versus**

671 **SCCA scores of phenotypic measures and their permutation test results of training and test**

672 **set.** Each permutation test result shows the null distribution of SCCA estimated by permutation test.

673 Dashed red line refers to the actual covariance of each mode.

674



675

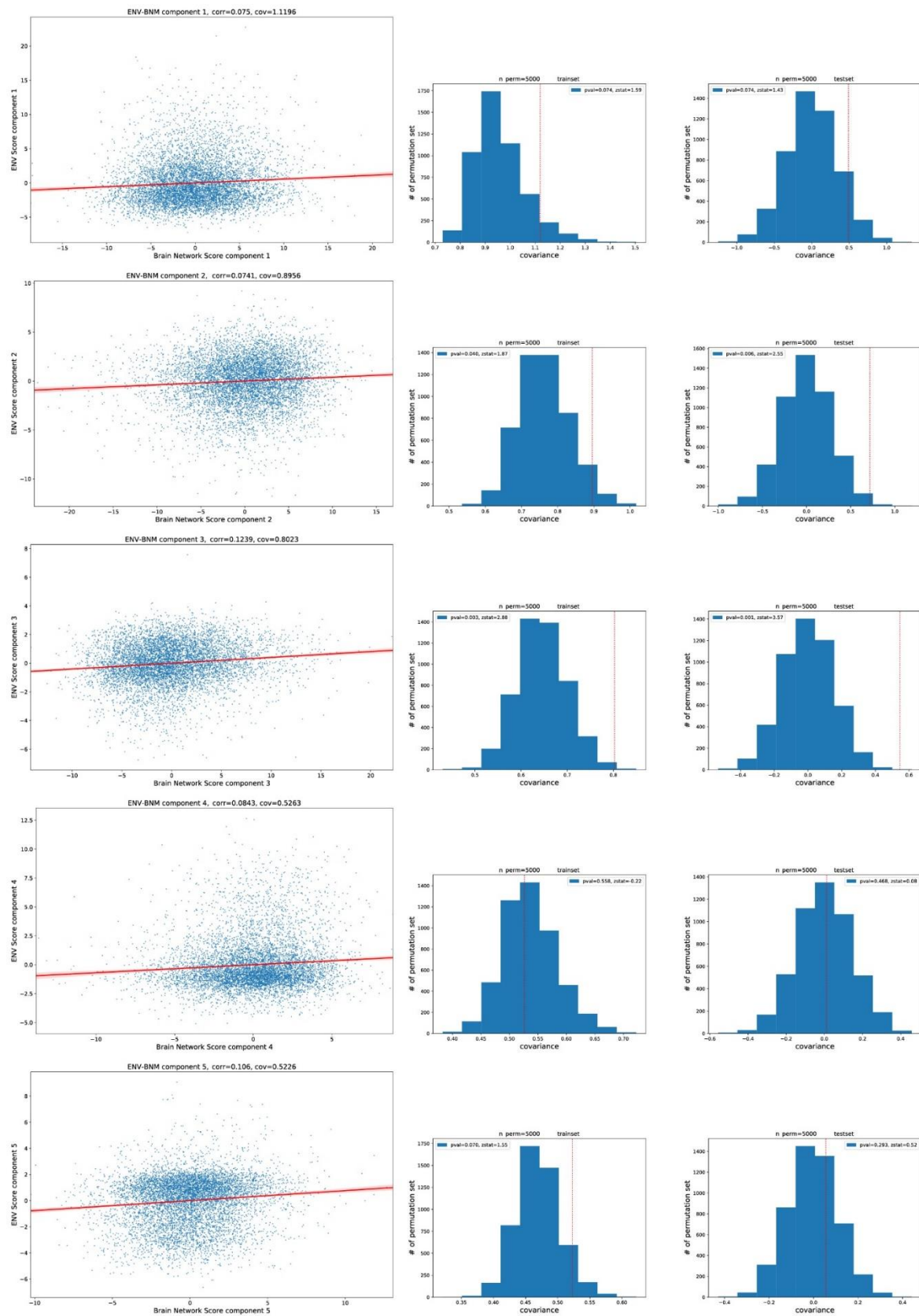
676 **Supplementary Figure 6. Sparse CCA loading patterns of brain network measures – phenotype**

677 **variables.** The left column presents the loading of each phenotype variable, while the right column

678 displays the loadings of global brain network measures and rich club coefficients. Each data point

679 represents the loading value of a specific variable and is color-coded based on its category. The error

680 bars indicate the 95% confidence interval of the loading, which was estimated using bootstrapping.
681 Gray-colored error bars indicate a 95% confidence interval that crosses 0. Yellow-colored error bars
682 indicate a 95% confidence interval that does not cross 0 but corresponds to a variable that is not
683 frequently selected by Sparse CCA. Red-colored error bars represent a 95% confidence interval that
684 does not cross 0 and indicates a variable that is frequently selected. Only the variables represented
685 by red error bars are presented in the main text.
686



687

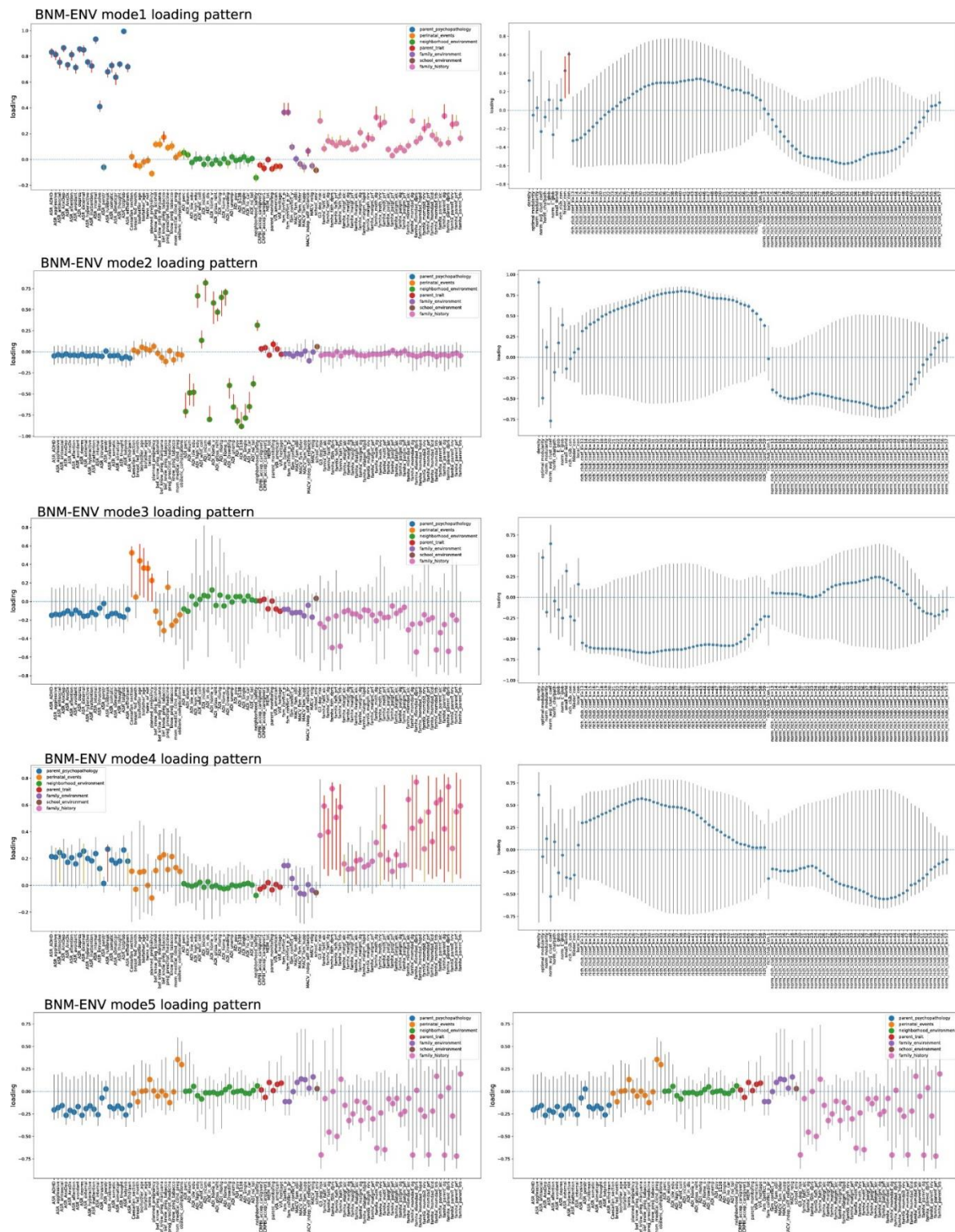
688 **Supplementary Figure 7. Scatter plots of SCCA scores of brain network measures versus**

689 **SCCA scores of environmental factors and their permutation test results of training and test**

690 **set.** Each permutation test result shows the null distribution of SCCA estimated by permutation test.

691 Dashed red line refers to the actual covariance of each mode.

692



693

694 **Supplementary Figure 8. Sparse CCA loading patterns of brain network measures –**

695 **environmental factors.** The left column presents the loading of each environmental variable, while

696 the right column displays the loadings of global brain network measures and rich club coefficients.

697 Each data point represents the loading value of a specific variable and is color-coded based on its

698 category. The error bars indicate the 95% confidence interval of the loading, which was estimated
699 using bootstrapping. Gray-colored error bars indicate a 95% confidence interval that crosses 0.
700 Yellow-colored error bars indicate a 95% confidence interval that does not cross 0 but corresponds to
701 a variable that is not frequently selected by Sparse CCA. Red-colored error bars represent a 95%
702 confidence interval that does not cross 0 and indicates a variable that is frequently selected. Only the
703 variables represented by red error bars are presented in the main text.

704

705 References

706

- 707 Achard, S., & Bullmore, E. (2007). Efficiency and cost of economical brain functional
708 networks. *PLoS Comput Biol*, 3(2), e17. <https://doi.org/10.1371/journal.pcbi.0030017>
- 709 Akiyama, M., Okada, Y., Kanai, M., Takahashi, A., Momozawa, Y., Ikeda, M., Iwata, N.,
710 Ikegawa, S., Hirata, M., Matsuda, K., Iwasaki, M., Yamaji, T., Sawada, N., Hachiya,
711 T., Tanno, K., Shimizu, A., Hozawa, A., Minegishi, N., Tsugane, S., . . . Kamatani, Y.
712 (2017). Genome-wide association study identifies 112 new loci for body mass index
713 in the Japanese population. *Nat Genet*, 49(10), 1458-1467.
714 <https://doi.org/10.1038/ng.3951>
- 715 Alexander-Bloch, A. F., Gogtay, N., Meunier, D., Birn, R., Clasen, L., Lalonde, F., Lenroot, R.,
716 Giedd, J., & Bullmore, E. T. (2010). Disrupted modularity and local connectivity of
717 brain functional networks in childhood-onset schizophrenia. *Front Syst Neurosci*, 4,
718 147. <https://doi.org/10.3389/fnsys.2010.00147>
- 719 Alnaes, D., Kaufmann, T., Marquand, A. F., Smith, S. M., & Westlye, L. T. (2020). Patterns of
720 sociocognitive stratification and perinatal risk in the child brain. *Proc Natl Acad Sci U*
721 *S A*, 117(22), 12419-12427. <https://doi.org/10.1073/pnas.2001517117>
- 722 Amare, A. T., Schubert, K. O., Klingler-Hoffmann, M., Cohen-Woods, S., & Baune, B. T.
723 (2017). The genetic overlap between mood disorders and cardiometabolic diseases:
724 a systematic review of genome wide and candidate gene studies. *Transl Psychiatry*,
725 7(1), e1007. <https://doi.org/10.1038/tp.2016.261>
- 726 Athey, S., Tibshirani, J., & Wager, S. (2019). Generalized random forests. *The Annals of*
727 *Statistics*, 47(2), 1148-1178, 1131. <https://doi.org/10.1214/18-AOS1709>
- 728 Baker, S. T., Lubman, D. I., Yucel, M., Allen, N. B., Whittle, S., Fulcher, B. D., Zalesky, A., &
729 Fornito, A. (2015). Developmental Changes in Brain Network Hub Connectivity in
730 Late Adolescence. *J Neurosci*, 35(24), 9078-9087.
731 <https://doi.org/10.1523/JNEUROSCI.5043-14.2015>
- 732 Barch, D., Pagliaccio, D., Belden, A., Harms, M. P., Gaffrey, M., Sylvester, C. M., Tillman, R.,
733 & Luby, J. (2016). Effect of Hippocampal and Amygdala Connectivity on the
734 Relationship Between Preschool Poverty and School-Age Depression. *Am J*
735 *Psychiatry*, 173(6), 625-634. <https://doi.org/10.1176/appi.ajp.2015.15081014>
- 736 Bassett, D. S., Bullmore, E. T., Meyer-Lindenberg, A., Apud, J. A., Weinberger, D. R., &
737 Coppola, R. (2009). Cognitive fitness of cost-efficient brain functional networks. *Proc*
738 *Natl Acad Sci U S A*, 106(28), 11747-11752.
739 <https://doi.org/10.1073/pnas.0903641106>
- 740 Bathelt, J., Gathercole, S. E., Butterfield, S., team, C., & Astle, D. E. (2018). Children's
741 academic attainment is linked to the global organization of the white matter
742 connectome. *Dev Sci*, 21(5), e12662. <https://doi.org/10.1111/desc.12662>
- 743 Bethlehem, R. A. I., Seidlitz, J., White, S. R., Vogel, J. W., Anderson, K. M., Adamson, C.,
744 Adler, S., Alexopoulos, G. S., Anagnostou, E., Areces-Gonzalez, A., Astle, D. E.,
745 Auyeung, B., Ayub, M., Bae, J., Ball, G., Baron-Cohen, S., Beare, R., Bedford, S. A.,
746 Benegal, V., . . . Alexander-Bloch, A. F. (2022). Brain charts for the human lifespan.
747 *Nature*, 604(7906), 525-533. <https://doi.org/10.1038/s41586-022-04554-y>
- 748 Binder, J. R., Desai, R. H., Graves, W. W., & Conant, L. L. (2009). Where is the semantic
749 system? A critical review and meta-analysis of 120 functional neuroimaging studies.
750 *Cereb Cortex*, 19(12), 2767-2796. <https://doi.org/10.1093/cercor/bhp055>
- 751 Bipolar, D., Schizophrenia Working Group of the Psychiatric Genomics Consortium.
752 Electronic address, d. r. v. e., Bipolar, D., & Schizophrenia Working Group of the

- 753 Psychiatric Genomics, C. (2018). Genomic Dissection of Bipolar Disorder and
754 Schizophrenia, Including 28 Subphenotypes. *Cell*, 173(7), 1705-1715 e1716.
755 <https://doi.org/10.1016/j.cell.2018.05.046>
- 756 Bullmore, E., & Sporns, O. (2012). The economy of brain network organization. *Nat Rev*
757 *Neurosci*, 13(5), 336-349. <https://doi.org/10.1038/nrn3214>
- 758 Bunge, S. A., & Wright, S. B. (2007). Neurodevelopmental changes in working memory and
759 cognitive control. *Curr Opin Neurobiol*, 17(2), 243-250.
760 <https://doi.org/10.1016/j.conb.2007.02.005>
- 761 Calamante, F., Tournier, J. D., Jackson, G. D., & Connelly, A. (2010). Track-density imaging
762 (TDI): super-resolution white matter imaging using whole-brain track-density
763 mapping. *Neuroimage*, 53(4), 1233-1243.
764 <https://doi.org/10.1016/j.neuroimage.2010.07.024>
- 765 Chen, T., Chen, Z., & Gong, Q. (2021). White Matter-Based Structural Brain Network of
766 Major Depression. *Adv Exp Med Biol*, 1305, 35-55. https://doi.org/10.1007/978-981-33-6044-0_3
- 768 Clay, H. B., Sullivan, S., & Konradi, C. (2011). Mitochondrial dysfunction and pathology in
769 bipolar disorder and schizophrenia. *Int J Dev Neurosci*, 29(3), 311-324.
770 <https://doi.org/10.1016/j.ijdevneu.2010.08.007>
- 771 Collin, G., Scholtens, L. H., Kahn, R. S., Hillegers, M. H. J., & van den Heuvel, M. P. (2017).
772 Affected Anatomical Rich Club and Structural-Functional Coupling in Young Offspring
773 of Schizophrenia and Bipolar Disorder Patients. *Biol Psychiatry*, 82(10), 746-755.
774 <https://doi.org/10.1016/j.biopsych.2017.06.013>
- 775 Conomos, M. P., Miller, M. B., & Thornton, T. A. (2015). Robust inference of population
776 structure for ancestry prediction and correction of stratification in the presence of
777 relatedness. *Genet Epidemiol*, 39(4), 276-293. <https://doi.org/10.1002/gepi.21896>
- 778 Conomos, M. P., Reiner, A. P., Weir, B. S., & Thornton, T. A. (2016). Model-free Estimation of
779 Recent Genetic Relatedness. *Am J Hum Genet*, 98(1), 127-148.
780 <https://doi.org/10.1016/j.ajhg.2015.11.022>
- 781 Cross-Disorder Group of the Psychiatric Genomics, C. (2013). Identification of risk loci with
782 shared effects on five major psychiatric disorders: a genome-wide analysis. *Lancet*,
783 381(9875), 1371-1379. [https://doi.org/10.1016/S0140-6736\(12\)62129-1](https://doi.org/10.1016/S0140-6736(12)62129-1)
- 784 Das, S., Forer, L., Schonherr, S., Sidore, C., Locke, A. E., Kwong, A., Vrieze, S. I., Chew, E.
785 Y., Levy, S., McGue, M., Schlessinger, D., Stambolian, D., Loh, P. R., Iacono, W. G.,
786 Swaroop, A., Scott, L. J., Cucca, F., Kronenberg, F., Boehnke, M., . . . Fuchsberger,
787 C. (2016). Next-generation genotype imputation service and methods. *Nat Genet*,
788 48(10), 1284-1287. <https://doi.org/10.1038/ng.3656>
- 789 Demontis, D., Walters, R. K., Martin, J., Mattheisen, M., Als, T. D., Agerbo, E., Baldursson,
790 G., Belliveau, R., Bybjerg-Grauholm, J., Baekvad-Hansen, M., Cerrato, F., Chambert,
791 K., Churchhouse, C., Dumont, A., Eriksson, N., Gandal, M., Goldstein, J. I., Grasby,
792 K. L., Grove, J., . . . Neale, B. M. (2019). Discovery of the first genome-wide
793 significant risk loci for attention deficit/hyperactivity disorder. *Nat Genet*, 51(1), 63-75.
794 <https://doi.org/10.1038/s41588-018-0269-7>
- 795 Desikan, R. S., Segonne, F., Fischl, B., Quinn, B. T., Dickerson, B. C., Blacker, D., Buckner,
796 R. L., Dale, A. M., Maguire, R. P., Hyman, B. T., Albert, M. S., & Killiany, R. J. (2006).
797 An automated labeling system for subdividing the human cerebral cortex on MRI
798 scans into gyral based regions of interest. *Neuroimage*, 31(3), 968-980.
799 <https://doi.org/10.1016/j.neuroimage.2006.01.021>
- 800 Fernandez-Cabello, S., Alnaes, D., van der Meer, D., Dahl, A., Holm, M., Kjelkenes, R.,
801 Maximov, I., Norbom, L. B., Pedersen, M. L., Voldsbekk, I., Andreassen, O. A., &
802 Westlye, L. T. (2022). Associations between brain imaging and polygenic scores of
803 mental health and educational attainment in children aged 9-11. *Neuroimage*, 263,
804 119611. <https://doi.org/10.1016/j.neuroimage.2022.119611>
- 805 Fornito, A., Zalesky, A., & Breakspear, M. (2015). The connectomics of brain disorders. *Nat*
806 *Rev Neurosci*, 16(3), 159-172. <https://doi.org/10.1038/nrn3901>

- 807 Ge, T., Chen, C. Y., Ni, Y., Feng, Y. A., & Smoller, J. W. (2019). Polygenic prediction via
808 Bayesian regression and continuous shrinkage priors. *Nat Commun*, *10*(1), 1776.
809 <https://doi.org/10.1038/s41467-019-09718-5>
- 810 Genomes Project, C., Auton, A., Brooks, L. D., Durbin, R. M., Garrison, E. P., Kang, H. M.,
811 Korb, J. O., Marchini, J. L., McCarthy, S., McVean, G. A., & Abecasis, G. R. (2015).
812 A global reference for human genetic variation. *Nature*, *526*(7571), 68-74.
813 <https://doi.org/10.1038/nature15393>
- 814 Greene, A. S., Shen, X., Noble, S., Horien, C., Hahn, C. A., Arora, J., Tokoglu, F., Spann, M.
815 N., Carrion, C. I., Barron, D. S., Sanacora, G., Srihari, V. H., Woods, S. W.,
816 Scheinost, D., & Constable, R. T. (2022). Brain-phenotype models fail for individuals
817 who defy sample stereotypes. *Nature*, *609*(7925), 109-118.
818 <https://doi.org/10.1038/s41586-022-05118-w>
- 819 Grove, J., Ripke, S., Als, T. D., Mattheisen, M., Walters, R. K., Won, H., Pallesen, J., Agerbo,
820 E., Andreassen, O. A., Anney, R., Awashti, S., Belliveau, R., Bettella, F., Buxbaum, J.
821 D., Bybjerg-Grauholm, J., Baekvad-Hansen, M., Cerrato, F., Chambert, K.,
822 Christensen, J. H., . . . Borglum, A. D. (2019). Identification of common genetic risk
823 variants for autism spectrum disorder. *Nat Genet*, *51*(3), 431-444.
824 <https://doi.org/10.1038/s41588-019-0344-8>
- 825 Hanson, J. L., Chandra, A., Wolfe, B. L., & Pollak, S. D. (2011). Association between income
826 and the hippocampus. *PLoS One*, *6*(5), e18712.
827 <https://doi.org/10.1371/journal.pone.0018712>
- 828 Hotelling, H. (1936). Relations between two sets of variates. *Biometrika*, *28*, 321-377.
829 <https://doi.org/10.1093/biomet/28.3-4.321>
- 830 Howard, D. M., Adams, M. J., Clarke, T. K., Hafferty, J. D., Gibson, J., Shiri, M., Coleman,
831 J. R. I., Hagenaars, S. P., Ward, J., Wigmore, E. M., Alloza, C., Shen, X., Barbu, M.
832 C., Xu, E. Y., Whalley, H. C., Marioni, R. E., Porteous, D. J., Davies, G., Deary, I.
833 J., . . . McIntosh, A. M. (2019). Genome-wide meta-analysis of depression identifies
834 102 independent variants and highlights the importance of the prefrontal brain
835 regions. *Nat Neurosci*, *22*(3), 343-352. <https://doi.org/10.1038/s41593-018-0326-7>
- 836 International Obsessive Compulsive Disorder Foundation Genetics, C., & Studies, O. C. D.
837 C. G. A. (2018). Revealing the complex genetic architecture of obsessive-compulsive
838 disorder using meta-analysis. *Mol Psychiatry*, *23*(5), 1181-1188.
839 <https://doi.org/10.1038/mp.2017.154>
- 840 Jansen, P. R., Watanabe, K., Stringer, S., Skene, N., Bryois, J., Hammerschlag, A. R., de
841 Leeuw, C. A., Benjamins, J. S., Munoz-Manchado, A. B., Nagel, M., Savage, J. E.,
842 Tiemeier, H., White, T., and Me Research, T., Tung, J. Y., Hinds, D. A., Vacic, V.,
843 Wang, X., Sullivan, P. F., . . . Posthuma, D. (2019). Genome-wide analysis of
844 insomnia in 1,331,010 individuals identifies new risk loci and functional pathways.
845 *Nat Genet*, *51*(3), 394-403. <https://doi.org/10.1038/s41588-018-0333-3>
- 846 Jarrard, L. E. (1993). On the role of the hippocampus in learning and memory in the rat.
847 *Behav Neural Biol*, *60*(1), 9-26. [https://doi.org/10.1016/0163-1047\(93\)90664-4](https://doi.org/10.1016/0163-1047(93)90664-4)
- 848 Jednorog, K., Altarelli, I., Monzalvo, K., Fluss, J., Dubois, J., Billard, C., Dehaene-Lambertz,
849 G., & Ramus, F. (2012). The influence of socioeconomic status on children's brain
850 structure. *PLoS One*, *7*(8), e42486. <https://doi.org/10.1371/journal.pone.0042486>
- 851 Jernigan, T. L., Brown, S. A., & Dowling, G. J. (2018). The Adolescent Brain Cognitive
852 Development Study. *J Res Adolesc*, *28*(1), 154-156.
853 <https://doi.org/10.1111/jora.12374>
- 854 Jeurissen, B., Descoteaux, M., Mori, S., & Leemans, A. (2019). Diffusion MRI fiber
855 tractography of the brain. *NMR Biomed*, *32*(4), e3785.
856 <https://doi.org/10.1002/nbm.3785>
- 857 Jung, R. E., & Haier, R. J. (2007). The Parieto-Frontal Integration Theory (P-FIT) of
858 intelligence: converging neuroimaging evidence. *Behav Brain Sci*, *30*(2), 135-154;
859 discussion 154-187. <https://doi.org/10.1017/S0140525X07001185>
- 860 Karlsson Linner, R., Biroli, P., Kong, E., Meddens, S. F. W., Wedow, R., Fontana, M. A.,

- 861 Lebreton, M., Tino, S. P., Abdellaoui, A., Hammerschlag, A. R., Nivard, M. G., Okbay,
862 A., Rietveld, C. A., Timshel, P. N., Trzaskowski, M., Vlaming, R., Zund, C. L., Bao, Y.,
863 Buzdugan, L., . . . Beauchamp, J. P. (2019). Genome-wide association analyses of
864 risk tolerance and risky behaviors in over 1 million individuals identify hundreds of
865 loci and shared genetic influences. *Nat Genet*, *51*(2), 245-257.
866 <https://doi.org/10.1038/s41588-018-0309-3>
- 867 Kim, D. J., Davis, E. P., Sandman, C. A., Glynn, L., Sporns, O., O'Donnell, B. F., & Hetrick,
868 W. P. (2019). Childhood poverty and the organization of structural brain connectome.
869 *Neuroimage*, *184*, 409-416. <https://doi.org/10.1016/j.neuroimage.2018.09.041>
- 870 Kim, D. J., Davis, E. P., Sandman, C. A., Sporns, O., O'Donnell, B. F., Buss, C., & Hetrick, W.
871 P. (2016). Children's intellectual ability is associated with structural network integrity.
872 *Neuroimage*, *124*(Pt A), 550-556. <https://doi.org/10.1016/j.neuroimage.2015.09.012>
- 873 Kim, K., Joo, Y. Y., Ahn, G., Wang, H. H., Moon, S. Y., Kim, H., Ahn, W. Y., & Cha, J. (2022).
874 The sexual brain, genes, and cognition: A machine-predicted brain sex score
875 explains individual differences in cognitive intelligence and genetic influence in young
876 children. *Hum Brain Mapp*, *43*(12), 3857-3872. <https://doi.org/10.1002/hbm.25888>
- 877 Kim, Y., Vadodaria, K. C., Lenkei, Z., Kato, T., Gage, F. H., Marchetto, M. C., & Santos, R.
878 (2019). Mitochondria, Metabolism, and Redox Mechanisms in Psychiatric Disorders.
879 *Antioxid Redox Signal*, *31*(4), 275-317. <https://doi.org/10.1089/ars.2018.7606>
- 880 Koenis, M. M., Brouwer, R. M., van den Heuvel, M. P., Mandl, R. C., van Soelen, I. L., Kahn,
881 R. S., Boomsma, D. I., & Hulshoff Pol, H. E. (2015). Development of the brain's
882 structural network efficiency in early adolescence: A longitudinal DTI twin study. *Hum*
883 *Brain Mapp*, *36*(12), 4938-4953. <https://doi.org/10.1002/hbm.22988>
- 884 Lam, M., Chen, C. Y., Li, Z., Martin, A. R., Bryois, J., Ma, X., Gaspar, H., Ikeda, M.,
885 Benyamin, B., Brown, B. C., Liu, R., Zhou, W., Guan, L., Kamatani, Y., Kim, S. W.,
886 Kubo, M., Kusumawardhani, A., Liu, C. M., Ma, H., . . . Huang, H. (2019).
887 Comparative genetic architectures of schizophrenia in East Asian and European
888 populations. *Nat Genet*, *51*(12), 1670-1678. [https://doi.org/10.1038/s41588-019-](https://doi.org/10.1038/s41588-019-0512-x)
889 [0512-x](https://doi.org/10.1038/s41588-019-0512-x)
- 890 Lee, J. J., Wedow, R., Okbay, A., Kong, E., Maghziyan, O., Zacher, M., Nguyen-Viet, T. A.,
891 Bowers, P., Sidorenko, J., Karlsson Linner, R., Fontana, M. A., Kundu, T., Lee, C., Li,
892 H., Li, R., Royer, R., Timshel, P. N., Walters, R. K., Willoughby, E. A., . . . Cesarini, D.
893 (2018). Gene discovery and polygenic prediction from a genome-wide association
894 study of educational attainment in 1.1 million individuals. *Nat Genet*, *50*(8), 1112-
895 1121. <https://doi.org/10.1038/s41588-018-0147-3>
- 896 Lett, T., Vogel, B. O., Ripke, S., Wackerhagen, C., Erk, S., Awasthi, S., Trubetskov, V.,
897 Brandl, E. J., Mohnke, S., Veer, I. M., Nothen, M. M., Rietschel, M., Degenhardt, F.,
898 Romanczuk-Seiferth, N., Witt, S. H., Banaschewski, T., Bokde, A., Buchel, C.,
899 Quinlan, E. B., . . . Consortium, I. (2020). Cortical Surfaces Mediate the Relationship
900 Between Polygenic Scores for Intelligence and General Intelligence. *Cerebral Cortex*,
901 *30*(4), 2708-2719. <https://doi.org/10.1093/cercor/bhz270>
- 902 Lim, S., Han, C. E., Uhlhaas, P. J., & Kaiser, M. (2015). Preferential detachment during
903 human brain development: age- and sex-specific structural connectivity in diffusion
904 tensor imaging (DTI) data. *Cereb Cortex*, *25*(6), 1477-1489.
905 <https://doi.org/10.1093/cercor/bht333>
- 906 Locke, A. E., Kahali, B., Berndt, S. I., Justice, A. E., Pers, T. H., Day, F. R., Powell, C.,
907 Vedantam, S., Buchkovich, M. L., Yang, J., Croteau-Chonka, D. C., Esko, T., Fall, T.,
908 Ferreira, T., Gustafsson, S., Kutalik, Z., Luan, J., Magi, R., Randall, J. C., . . .
909 Speliotes, E. K. (2015). Genetic studies of body mass index yield new insights for
910 obesity biology. *Nature*, *518*(7538), 197-206. <https://doi.org/10.1038/nature14177>
- 911 Loh, P. R., Danecek, P., Palamara, P. F., Fuchsberger, C., Y, A. R., H, K. F., Schoenherr, S.,
912 Forer, L., McCarthy, S., Abecasis, G. R., Durbin, R., & A, L. P. (2016). Reference-
913 based phasing using the Haplotype Reference Consortium panel. *Nat Genet*, *48*(11),
914 1443-1448. <https://doi.org/10.1038/ng.3679>

- 915 Luna, B., Padmanabhan, A., & O'Hearn, K. (2010). What has fMRI told us about the
916 development of cognitive control through adolescence? *Brain Cogn*, 72(1), 101-113.
917 <https://doi.org/10.1016/j.bandc.2009.08.005>
- 918 Ma, J., Kang, H. J., Kim, J. Y., Jeong, H. S., Im, J. J., Namgung, E., Kim, M. J., Lee, S., Kim,
919 T. D., Oh, J. K., Chung, Y. A., Lyoo, I. K., Lim, S. M., & Yoon, S. (2017). Network
920 attributes underlying intellectual giftedness in the developing brain. *Sci Rep*, 7(1),
921 11321. <https://doi.org/10.1038/s41598-017-11593-3>
- 922 Marek, S., Tervo-Clemmens, B., Calabro, F. J., Montez, D. F., Kay, B. P., Hatoum, A. S.,
923 Donohue, M. R., Foran, W., Miller, R. L., Hendrickson, T. J., Malone, S. M., Kandala,
924 S., Feczko, E., Miranda-Dominguez, O., Graham, A. M., Earl, E. A., Perrone, A. J.,
925 Cordova, M., Doyle, O., . . . Dosenbach, N. U. F. (2022). Reproducible brain-wide
926 association studies require thousands of individuals. *Nature*, 603(7902), 654-660.
927 <https://doi.org/10.1038/s41586-022-04492-9>
- 928 Masic, B., Betzel, R. F., de Reus, M. A., van den Heuvel, M. P., Berman, M. G., McIntosh, A.
929 R., & Sporns, O. (2016). Network-Level Structure-Function Relationships in Human
930 Neocortex. *Cereb Cortex*, 26(7), 3285-3296. <https://doi.org/10.1093/cercor/bhw089>
- 931 Modabbernia, A., Janiri, D., Doucet, G. E., Reichenberg, A., & Frangou, S. (2021).
932 Multivariate Patterns of Brain-Behavior-Environment Associations in the Adolescent
933 Brain and Cognitive Development Study. *Biol Psychiatry*, 89(5), 510-520.
934 <https://doi.org/10.1016/j.biopsych.2020.08.014>
- 935 Mowinckel, A. M., & Vidal-Pineiro, D. (2020). Visualization of Brain Statistics With R
936 Packages ggseg and ggseg3d. *Advances in Methods and Practices in Psychological
937 Science*, 3(4), 466-483. <https://doi.org/10.1177/2515245920928009>
- 938 Nagel, M., Jansen, P. R., Stringer, S., Watanabe, K., de Leeuw, C. A., Bryois, J., Savage, J.
939 E., Hammerschlag, A. R., Skene, N. G., Munoz-Manchado, A. B., andMe Research,
940 T., White, T., Tiemeier, H., Linnarsson, S., Hjerling-Leffler, J., Polderman, T. J. C.,
941 Sullivan, P. F., van der Sluis, S., & Posthuma, D. (2018). Meta-analysis of genome-
942 wide association studies for neuroticism in 449,484 individuals identifies novel
943 genetic loci and pathways. *Nat Genet*, 50(7), 920-927.
944 <https://doi.org/10.1038/s41588-018-0151-7>
- 945 Namkung, H., Kim, S. H., & Sawa, A. (2017). The Insula: An Underestimated Brain Area in
946 Clinical Neuroscience, Psychiatry, and Neurology. *Trends Neurosci*, 40(4), 200-207.
947 <https://doi.org/10.1016/j.tins.2017.02.002>
- 948 Nievergelt, C. M., Maihofer, A. X., Klengel, T., Atkinson, E. G., Chen, C. Y., Choi, K. W.,
949 Coleman, J. R. I., Dalvie, S., Duncan, L. E., Gelernter, J., Levey, D. F., Logue, M. W.,
950 Polimanti, R., Provost, A. C., Ratanatharathorn, A., Stein, M. B., Torres, K., Aiello, A.
951 E., Almli, L. M., . . . Koenen, K. C. (2019). International meta-analysis of PTSD
952 genome-wide association studies identifies sex- and ancestry-specific genetic risk
953 loci. *Nat Commun*, 10(1), 4558. <https://doi.org/10.1038/s41467-019-12576-w>
- 954 Okbay, A., Baselmans, B. M., De Neve, J. E., Turley, P., Nivard, M. G., Fontana, M. A.,
955 Meddens, S. F., Linner, R. K., Rietveld, C. A., Derringer, J., Gratten, J., Lee, J. J., Liu,
956 J. Z., de Vlaming, R., Ahluwalia, T. S., Buchwald, J., Cavadino, A., Frazier-Wood, A.
957 C., Furlotte, N. A., . . . Cesarini, D. (2016). Genetic variants associated with
958 subjective well-being, depressive symptoms, and neuroticism identified through
959 genome-wide analyses. *Nat Genet*, 48(6), 624-633. <https://doi.org/10.1038/ng.3552>
- 960 Otowa, T., Hek, K., Lee, M., Byrne, E. M., Mirza, S. S., Nivard, M. G., Bigdeli, T., Aggen, S.
961 H., Adkins, D., Wolen, A., Fanous, A., Keller, M. C., Castelao, E., Kutalik, Z., der
962 Auwera, S. V., Homuth, G., Nauck, M., Teumer, A., Milaneschi, Y., . . . Hettema, J. M.
963 (2016). Meta-analysis of genome-wide association studies of anxiety disorders. *Mol
964 Psychiatry*, 21(10), 1485. <https://doi.org/10.1038/mp.2016.11>
- 965 Pasman, J. A., Verweij, K. J. H., Gerring, Z., Stringer, S., Sanchez-Roige, S., Treur, J. L.,
966 Abdellaoui, A., Nivard, M. G., Baselmans, B. M. L., Ong, J. S., Ip, H. F., van der Zee,
967 M. D., Bartels, M., Day, F. R., Fontanillas, P., Elson, S. L., andMe Research, T., de
968 Wit, H., Davis, L. K., . . . Vink, J. M. (2019). Author Correction: GWAS of lifetime

- 969 cannabis use reveals new risk loci, genetic overlap with psychiatric traits, and a
970 causal effect of schizophrenia liability. *Nat Neurosci*, 22(7), 1196.
971 <https://doi.org/10.1038/s41593-019-0402-7>
- 972 Paus, T., Keshavan, M., & Giedd, J. N. (2008). Why do many psychiatric disorders emerge
973 during adolescence? *Nat Rev Neurosci*, 9(12), 947-957.
974 <https://doi.org/10.1038/nrn2513>
- 975 Perry, A., Roberts, G., Mitchell, P. B., & Breakspear, M. (2019). Correction: Connectomics of
976 bipolar disorder: a critical review, and evidence for dynamic instabilities within
977 interoceptive networks. *Mol Psychiatry*, 24(9), 1398. <https://doi.org/10.1038/s41380-018-0327-7>
- 978
- 979 Phelps, E. A. (2004). Human emotion and memory: interactions of the amygdala and
980 hippocampal complex. *Curr Opin Neurobiol*, 14(2), 198-202.
981 <https://doi.org/10.1016/j.conb.2004.03.015>
- 982 Rezin, G. T., Amboni, G., Zugno, A. I., Quevedo, J., & Streck, E. L. (2009). Mitochondrial
983 dysfunction and psychiatric disorders. *Neurochem Res*, 34(6), 1021-1029.
984 <https://doi.org/10.1007/s11064-008-9865-8>
- 985 Rodevand, L., Bahrami, S., Frei, O., Chu, Y., Shadrin, A., O'Connell, K. S., Smeland, O. B.,
986 Elvsashagen, T., Hindley, G. F. L., Djurovic, S., Dale, A. M., Lagerberg, T. V., Steen,
987 N. E., & Andreassen, O. A. (2021). Extensive bidirectional genetic overlap between
988 bipolar disorder and cardiovascular disease phenotypes. *Transl Psychiatry*, 11(1),
989 407. <https://doi.org/10.1038/s41398-021-01527-z>
- 990 Rubin, R. D., Watson, P. D., Duff, M. C., & Cohen, N. J. (2014). The role of the hippocampus
991 in flexible cognition and social behavior. *Front Hum Neurosci*, 8, 742.
992 <https://doi.org/10.3389/fnhum.2014.00742>
- 993 Rubinov, M., & Sporns, O. (2010). Complex network measures of brain connectivity: uses
994 and interpretations. *Neuroimage*, 52(3), 1059-1069.
995 <https://doi.org/10.1016/j.neuroimage.2009.10.003>
- 996 Rudie, J. D., Brown, J. A., Beck-Pancer, D., Hernandez, L. M., Dennis, E. L., Thompson, P.
997 M., Bookheimer, S. Y., & Dapretto, M. (2012). Altered functional and structural brain
998 network organization in autism. *Neuroimage Clin*, 2, 79-94.
999 <https://doi.org/10.1016/j.nicl.2012.11.006>
- 1000 Savage, J. E., Jansen, P. R., Stringer, S., Watanabe, K., Bryois, J., de Leeuw, C. A., Nagel,
1001 M., Awasthi, S., Barr, P. B., Coleman, J. R. I., Grasby, K. L., Hammerschlag, A. R.,
1002 Kaminski, J. A., Karlsson, R., Krapohl, E., Lam, M., Nygaard, M., Reynolds, C. A.,
1003 Trampush, J. W., . . . Posthuma, D. (2018). Genome-wide association meta-analysis
1004 in 269,867 individuals identifies new genetic and functional links to intelligence. *Nat*
1005 *Genet*, 50(7), 912-919. <https://doi.org/10.1038/s41588-018-0152-6>
- 1006 Seghier, M. L. (2013). The angular gyrus: multiple functions and multiple subdivisions.
1007 *Neuroscientist*, 19(1), 43-61. <https://doi.org/10.1177/1073858412440596>
- 1008 Shao, L., Martin, M. V., Watson, S. J., Schatzberg, A., Akil, H., Myers, R. M., Jones, E. G.,
1009 Bunney, W. E., & Vawter, M. P. (2008). Mitochondrial involvement in psychiatric
1010 disorders. *Ann Med*, 40(4), 281-295. <https://doi.org/10.1080/07853890801923753>
- 1011 Shen, H., Gelaye, B., Huang, H., Rondon, M. B., Sanchez, S., & Duncan, L. E. (2020).
1012 Polygenic prediction and GWAS of depression, PTSD, and suicidal ideation/self-
1013 harm in a Peruvian cohort. *Neuropsychopharmacology*, 45(10), 1595-1602.
1014 <https://doi.org/10.1038/s41386-020-0603-5>
- 1015 Smith, R. E., Tournier, J. D., Calamante, F., & Connelly, A. (2013). SIFT: Spherical-
1016 deconvolution informed filtering of tractograms. *Neuroimage*, 67, 298-312.
1017 <https://doi.org/10.1016/j.neuroimage.2012.11.049>
- 1018 Smith, S. M., Nichols, T. E., Vidaurre, D., Winkler, A. M., Behrens, T. E., Glasser, M. F.,
1019 Ugurbil, K., Barch, D. M., Van Essen, D. C., & Miller, K. L. (2015). A positive-negative
1020 mode of population covariation links brain connectivity, demographics and behavior.
1021 *Nat Neurosci*, 18(11), 1565-1567. <https://doi.org/10.1038/nn.4125>
- 1022 Sotiropoulos, S. N., & Zalesky, A. (2019). Building connectomes using diffusion MRI: why,

- 1023 how and but. *NMR Biomed*, 32(4), e3752. <https://doi.org/10.1002/nbm.3752>
- 1024 Stahl, E. A., Breen, G., Forstner, A. J., McQuillin, A., Ripke, S., Trubetskov, V., Mattheisen,
1025 M., Wang, Y., Coleman, J. R. I., Gaspar, H. A., de Leeuw, C. A., Steinberg, S.,
1026 Pavlidis, J. M. W., Trzaskowski, M., Byrne, E. M., Pers, T. H., Holmans, P. A.,
1027 Richards, A. L., Abbott, L., . . . Bipolar Disorder Working Group of the Psychiatric
1028 Genomics, C. (2019). Genome-wide association study identifies 30 loci associated
1029 with bipolar disorder. *Nat Genet*, 51(5), 793-803. [https://doi.org/10.1038/s41588-019-](https://doi.org/10.1038/s41588-019-0397-8)
1030 [0397-8](https://doi.org/10.1038/s41588-019-0397-8)
- 1031 Suprano, I., Kocevar, G., Stamile, C., Hannoun, S., Fournier, P., Revol, O., Nusbaum, F., &
1032 Sappey-Marini, D. (2020). White matter microarchitecture and structural network
1033 integrity correlate with children intelligence quotient. *Sci Rep*, 10(1), 20722.
1034 <https://doi.org/10.1038/s41598-020-76528-x>
- 1035 Sweatt, J. D. (2004). Hippocampal function in cognition. *Psychopharmacology (Berl)*, 174(1),
1036 99-110. <https://doi.org/10.1007/s00213-004-1795-9>
- 1037 Tamnes, C. K., Roalf, D. R., Goddings, A. L., & Lebel, C. (2018). Diffusion MRI of white
1038 matter microstructure development in childhood and adolescence: Methods,
1039 challenges and progress. *Dev Cogn Neurosci*, 33, 161-175.
1040 <https://doi.org/10.1016/j.dcn.2017.12.002>
- 1041 Taquet, M., Smith, S. M., Prohl, A. K., Peters, J. M., Warfield, S. K., Scherrer, B., & Harrison,
1042 P. J. (2021). A structural brain network of genetic vulnerability to psychiatric illness.
1043 *Mol Psychiatry*, 26(6), 2089-2100. <https://doi.org/10.1038/s41380-020-0723-7>
- 1044 Tooley, U. A., Mackey, A. P., Ciric, R., Ruparel, K., Moore, T. M., Gur, R. C., Gur, R. E.,
1045 Satterthwaite, T. D., & Bassett, D. S. (2020). Associations between Neighborhood
1046 SES and Functional Brain Network Development. *Cereb Cortex*, 30(1), 1-19.
1047 <https://doi.org/10.1093/cercor/bhz066>
- 1048 Torkamani, A., Wineinger, N. E., & Topol, E. J. (2018). The personal and clinical utility of
1049 polygenic risk scores. *Nat Rev Genet*, 19(9), 581-590.
1050 <https://doi.org/10.1038/s41576-018-0018-x>
- 1051 Tournier, J. D., Calamante, F., & Connelly, A. (2007). Robust determination of the fibre
1052 orientation distribution in diffusion MRI: non-negativity constrained super-resolved
1053 spherical deconvolution. *Neuroimage*, 35(4), 1459-1472.
1054 <https://doi.org/10.1016/j.neuroimage.2007.02.016>
- 1055 Tournier, J. D., Smith, R., Raffelt, D., Tabbara, R., Dhollander, T., Pietsch, M., Christiaens,
1056 D., Jeurissen, B., Yeh, C. H., & Connelly, A. (2019). MRtrix3: A fast, flexible and open
1057 software framework for medical image processing and visualisation. *Neuroimage*,
1058 202, 116137. <https://doi.org/10.1016/j.neuroimage.2019.116137>
- 1059 van den Heuvel, M. P., & Fornito, A. (2014). Brain networks in schizophrenia. *Neuropsychol*
1060 *Rev*, 24(1), 32-48. <https://doi.org/10.1007/s11065-014-9248-7>
- 1061 van den Heuvel, M. P., & Sporns, O. (2011). Rich-club organization of the human
1062 connectome. *J Neurosci*, 31(44), 15775-15786.
1063 <https://doi.org/10.1523/JNEUROSCI.3539-11.2011>
- 1064 van den Heuvel, M. P., Sporns, O., Collin, G., Scheewe, T., Mandl, R. C., Cahn, W., Goni, J.,
1065 Hulshoff Pol, H. E., & Kahn, R. S. (2013). Abnormal rich club organization and
1066 functional brain dynamics in schizophrenia. *JAMA Psychiatry*, 70(8), 783-792.
1067 <https://doi.org/10.1001/jamapsychiatry.2013.1328>
- 1068 van den Heuvel, M. P., van Soelen, I. L., Stam, C. J., Kahn, R. S., Boomsma, D. I., &
1069 Hulshoff Pol, H. E. (2013). Genetic control of functional brain network efficiency in
1070 children. *Eur Neuropsychopharmacol*, 23(1), 19-23.
1071 <https://doi.org/10.1016/j.euroneuro.2012.06.007>
- 1072 van Wijk, B. C., Stam, C. J., & Daffertshofer, A. (2010). Comparing brain networks of
1073 different size and connectivity density using graph theory. *PLoS One*, 5(10), e13701.
1074 <https://doi.org/10.1371/journal.pone.0013701>
- 1075 Visser, M., Jefferies, E., Embleton, K. V., & Lambon Ralph, M. A. (2012). Both the middle
1076 temporal gyrus and the ventral anterior temporal area are crucial for multimodal

1077 semantic processing: distortion-corrected fMRI evidence for a double gradient of
1078 information convergence in the temporal lobes. *J Cogn Neurosci*, 24(8), 1766-1778.
1079 https://doi.org/10.1162/jocn_a_00244

1080 Walters, R. K., Polimanti, R., Johnson, E. C., McClintick, J. N., Adams, M. J., Adkins, A. E.,
1081 Aliev, F., Bacanu, S. A., Batzler, A., Bertelsen, S., Biernacka, J. M., Bigdeli, T. B.,
1082 Chen, L. S., Clarke, T. K., Chou, Y. L., Degenhardt, F., Docherty, A. R., Edwards, A.
1083 C., Fontanillas, P., . . . Agrawal, A. (2018). Transancestral GWAS of alcohol
1084 dependence reveals common genetic underpinnings with psychiatric disorders. *Nat*
1085 *Neurosci*, 21(12), 1656-1669. <https://doi.org/10.1038/s41593-018-0275-1>

1086 Wang, H. T., Smallwood, J., Mourao-Miranda, J., Xia, C. H., Satterthwaite, T. D., Bassett, D.
1087 S., & Bzdok, D. (2020). Finding the needle in a high-dimensional haystack: Canonical
1088 correlation analysis for neuroscientists. *Neuroimage*, 216, 116745.
1089 <https://doi.org/10.1016/j.neuroimage.2020.116745>

1090 Watson, H. J., Yilmaz, Z., Thornton, L. M., Hubel, C., Coleman, J. R. I., Gaspar, H. A.,
1091 Bryois, J., Hinney, A., Leppa, V. M., Mattheisen, M., Medland, S. E., Ripke, S., Yao,
1092 S., Giusti-Rodriguez, P., Anorexia Nervosa Genetics, I., Hanscombe, K. B., Purves,
1093 K. L., Eating Disorders Working Group of the Psychiatric Genomics, C., Adan, R. A.
1094 H., . . . Bulik, C. M. (2019). Genome-wide association study identifies eight risk loci
1095 and implicates metabo-psychiatric origins for anorexia nervosa. *Nat Genet*, 51(8),
1096 1207-1214. <https://doi.org/10.1038/s41588-019-0439-2>

1097 Witten, D. M., Tibshirani, R., & Hastie, T. (2009). A penalized matrix decomposition, with
1098 applications to sparse principal components and canonical correlation analysis.
1099 *Biostatistics*, 10(3), 515-534. <https://doi.org/10.1093/biostatistics/kxp008>

1100 Wray, N. R., Ripke, S., Mattheisen, M., Trzaskowski, M., Byrne, E. M., Abdellaoui, A.,
1101 Adams, M. J., Agerbo, E., Air, T. M., Andlauer, T. M. F., Bacanu, S. A., Baekvad-
1102 Hansen, M., Beekman, A. F. T., Bigdeli, T. B., Binder, E. B., Blackwood, D. R. H.,
1103 Bryois, J., Buttenschon, H. N., Bybjerg-Grauholm, J., . . . Major Depressive Disorder
1104 Working Group of the Psychiatric Genomics, C. (2018). Genome-wide association
1105 analyses identify 44 risk variants and refine the genetic architecture of major
1106 depression. *Nat Genet*, 50(5), 668-681. <https://doi.org/10.1038/s41588-018-0090-3>

1107 Xia, C. H., Ma, Z., Ciric, R., Gu, S., Betzel, R. F., Kaczkurkin, A. N., Calkins, M. E., Cook, P.
1108 A., Garcia de la Garza, A., Vandekar, S. N., Cui, Z., Moore, T. M., Roalf, D. R.,
1109 Ruparel, K., Wolf, D. H., Davatzikos, C., Gur, R. C., Gur, R. E., Shinohara, R. T., . . .
1110 Satterthwaite, T. D. (2018). Linked dimensions of psychopathology and connectivity
1111 in functional brain networks. *Nat Commun*, 9(1), 3003.
1112 <https://doi.org/10.1038/s41467-018-05317-y>

1113 Xu, L., Skoularidou, M., Cuesta-Infante, A., & Veeramachaneni, K. (2019). Modeling tabular
1114 data using conditional gan. *Advances in neural information processing systems*, 32.

1115 Zuccoli, G. S., Saia-Cereda, V. M., Nascimento, J. M., & Martins-de-Souza, D. (2017). The
1116 Energy Metabolism Dysfunction in Psychiatric Disorders Postmortem Brains: Focus
1117 on Proteomic Evidence. *Front Neurosci*, 11, 493.
1118 <https://doi.org/10.3389/fnins.2017.00493>